Addition of interleukin-2 overcomes resistance to neoadjuvant CTLA4 and PD1 blockade in ex vivo patient tumors

Kaptein, P.; Jacoberger-Foissac, C.; Dimitriadis, P.; Voabil, P.; Bruijn, M. de; Brokamp, S.; ... ; Teng, M.W.L.

CANCER

Addition of interleukin-2 overcomes resistance to neoadjuvant CTLA4 and PD1 blockade in ex vivo patient tumors

Paulien Kaptein[1]†, Celia Jacoberger-Foissac[2]†, Petros Dimitriadis[3]†, Paula Voabil[1], Marjolein de Bruijn[1], Simone Brokamp[1], Irene Reijers[3], Judith Versluis[3], Gahyathiri Nallan[2], Hannah Triscott[2,4], Elizabeth McDonald[2], Joshua Tay[2], Georgina V. Long[5,6,7], Christian U. Blank[1,3]*‡, Daniela S. Thommen[1]‡, Michele W.L. Teng[2,4]‡

Neoadjuvant immunotherapy with anti-cytotoxic T lymphocyte–associated protein 4 (CTLA4) + anti–programmed cell death protein 1 (PD1) monoclonal antibodies has demonstrated remarkable pathological responses and relapse-free survival in ~80% of patients with clinically detectable stage III melanoma. However, about 20% of the treated patients do not respond. In pretreatment biopsies of patients with melanoma, we found that resistance to neoadjuvant CTLA4 + PD1 blockade was associated with a low CD4/interleukin-2 (IL-2) gene signature. Ex vivo, addition of IL-2 to CTLA4 + PD1 blockade induced T cell activation and deep immunological responses in anti-CTLA4 + anti-PD1–resistant human tumor specimens. In the 4T1.2 breast cancer mouse model of neoadjuvant immunotherapy, triple combination of anti-CTLA4 + anti-PD1 + IL-2 cured almost twice as many mice as compared with dual checkpoint inhibitor therapy. This improved efficacy was due to the expansion of tumor-specific CD8$^+$ T cells and improved proinflammatory cytokine polyfunctionality of both CD4$^+$ and CD8$^+$ T effector cells and regulatory T cells. Depletion studies suggested that CD4$^+$ T cells were critical for priming of CD8$^+$ T cell immunity against 4T1.2 and helped in the expansion of tumor-specific CD8$^+$ T cells early after neoadjuvant triple immunotherapy. Our results suggest that the addition of IL-2 can overcome resistance to neoadjuvant anti-CTLA4 + anti-PD1, providing the rationale for testing this combination as a neoadjuvant therapy in patients with early-stage cancer.

INTRODUCTION

Neoadjuvant application of immune checkpoint inhibitors (ICIs) is currently the most promising immunotherapy for cancer treatment (1). This is based on the idea that in early-stage disease, responses to checkpoint inhibition are more frequent, likely due to reduced tumor-mediated immune suppression (2), and that tumor-specific T cell expansion is greater when ICI is administered before, compared with after, complete surgical resection of the tumor. This has been demonstrated preclinically using the orthotopic 4T1.2 triple-negative breast tumor mouse allograft model, which to date represents the best model where surgery and lethal metastases can be assessed in the context of neoadjuvant versus adjuvant therapy in a robust and timely manner (3). Clinically, proof of concept that neoadjuvant compared with adjuvant immunotherapy is more efficacious was demonstrated in a small trial in patients with melanoma (4). In early-stage melanoma, several trials have reported 30 to 33% pathologic response rates (pRR) for neoadjuvant PD1 blockade (5, 6) and 71 to 80% pRR for the combination of neoadjuvant CTLA4 + PD1 blockade (7, 8). This high pRR in the combination ICI-treated group is unparalleled and associated with long-term relapse-free survival

(RFS) (9). Among the patients who achieved a pathological complete response (pCR) or near pCR, hardly any patients relapsed, suggesting this parameter was a strong surrogate for long-term outcome (9). First attempts to characterize high-risk stage III patients with melanoma responding to neoadjuvant CTLA4 + PD1 blockade identified tumor mutational burden (TMB) and an interferon-γ (IFN-γ) signature to be independent baseline predictors of response (4, 10). Extended human RNA signature analyses have shown that pRR and RFS were also associated with a T cell signature and a basic leucine zipper transcription factor ATF-like 3 (BATF3) (11, 12). Preclinically, using T cell depletion of wild-type (WT) mice or Batf3$^{-/-}$ mice bearing 4T1.2 tumors, T cells and Batf3 lineage–derived dendritic cells (DCs) were found to be critical for the efficacy of neoadjuvant immunotherapy (3, 12). Overall, these findings are in agreement with neoadjuvant immunotherapy trials in patients with melanoma, showing that patients whose tumors have low IFN-γ and TMB signatures or display a low T cell and BATF3 signature are likely not to respond (4, 10, 12). Hence, this raises the question of whether alternative or additional therapy to neoadjuvant CTLA4 + PD1 blockade could convert nonresponders into responders.

The effective priming of a cytotoxic T cell response is dependent on CD4$^+$ T helper 1 (T$_H$1) cells, which increase DC antigen presentation and costimulatory capacity (13). Activated CD4 T$_H$1 cells are a major source of interleukin-2 (IL-2), which has known proactivation and proliferative functions on T cells (14). IL-2 also improves the chemotactic responsiveness of T cells (15) and was recently shown in mice and humans to induce DC expansion and activation through cytokines produced by IL-2–activated T cells (16). Although the addition of IL-2 in combination with other immunotherapies has demonstrated utility in mouse models of cancer mimicking advanced

[1]Division of Molecular Oncology and Immunology, Netherlands Cancer Institute, Amsterdam 1066 CX, Netherlands. [2]QIMR Berghofer Medical Research Institute, Brisbane, Queensland 4006, Australia. [3]Department of Medical Oncology, Netherlands Cancer Institute, Amsterdam 1066 CX, Netherlands. [4]School of Medicine, University of Queensland, Herston, Queensland 4006, Australia. [5]Melanoma Institute Australia, University of Sydney, Sydney 2006, Australia. [6]Faculty of Medicine and Health, University of Sydney, Sydney 2006, Australia. [7]Royal North Shore and Mater Hospitals, Sydney 2065, Australia.
*Corresponding author. Email: c.blank@nki.nl
†These authors share first authorship.
‡These authors share senior authorship.

disease and in small clinical trials to treat late-stage disease (*17–19*), it is unclear whether the use of IL-2 in the neoadjuvant setting will also be beneficial. Here in this study, we assessed whether resistance to neoadjuvant CTLA4 + PD1 blockade was associated with a low CD4/IL-2 signature, whether this impaired response was reversed by the addition of IL-2, and whether the addition of IL-2 further improved the outcome of neoadjuvant dual checkpoint inhibition.

RESULTS

A CD4/IL-2 gene signature is associated with response to neoadjuvant ipilimumab + nivolumab

To investigate a potential association between the presence of CD4+ T cells, IL-2, and neoadjuvant treatment response, we generated a CD4/IL-2 gene expression signature consisting of 10 well-known CD4 T cell–associated genes [*IL-2*, *CD4*, inducible T cell costimulator (*ICOS*), Eomesodermin (*EOMES*), *IL-21R*, *IL-2RA*, *IL-2RB*, *IL-2RG*, and *CD48*]. We performed an analysis of pretreatment tumor biopsies from patients with stage III melanoma from the PRADO (Personalized Response-driven Adjuvant Combination) extension cohort (*n* = 79), in which patients were treated with two courses of ipilimumab (anti-CTLA4, 1 mg/kg) + nivolumab (anti-PD1, 3 mg/kg) (NCT02977052) (table S1). Using this cohort as our training dataset, we found that a high CD4/IL-2 gene signature was associated with pathological response (53/79, 67%) as defined using the International Neoadjuvant Melanoma Consortium (INMC) response assessment criteria (*20*). Using the upper tertile of the CD4/IL-2 signature scores as threshold, we found the majority of patients (25/27, 93%) with a high CD4/IL-2 signature score responded to neoadjuvant combination immunotherapy (Fig. 1). In contrast, for the two-thirds of patients below the threshold and thus defined as having a low CD4/IL-2 signature score, only 28 of 52 (54%) patients responded (Fig. 1). We next validated the CD4/IL-2 signature score using NanoString data from an additional independent cohort of patients with stage III melanoma treated with neoadjuvant ipilimumab + nivolumab (OpACIN-neo, *n* = 64) (table S2) (*7*). Again, we found that the majority of patients (19/21, 90%) with a high CD4/IL-2 signature responded to neoadjuvant immunotherapy, whereas only 28 of 43 (65%) patients with a low CD4/IL-2 signature score responded (fig. S1A). Previously, we have shown that both a T cell signature and a BATF3 signature correlated with response to neoadjuvant immunotherapy (*4*, *12*). To compare the CD4/IL-2 signature to the T cell and BATF3 signatures, we analyzed the CD8 signature (*21*) and, as the NanoString PanCancer panel used in this study does not include all of the genes, a panel of subset genes from the BATF3 signature (*22*). We found that the CD4/IL-2 signature correlated with these other signatures (Fig. 1, indicated on top, and fig. S1, B and C), suggesting that nonresponse to neoadjuvant immunotherapy might relate to a defect at the stage of early immune activation.

Addition of IL-2 to combination checkpoint blockade induces immunological responses in human tumor explants resistant to anti-CTLA4 + anti-PD1

To examine the potential benefit of adding IL-2 to CTLA4 + PD1 blockade, we tested this triple combination therapy in our ex vivo tumor fragment model. We previously have shown that addition of anti-PD1 monoclonal antibodies to patient-derived tumor fragments (PDTFs) induces T cell activation and early immunological responses that can predict clinical response to PD1 blockade (*23*). In this

PDTF platform, human tumor tissue obtained from surgical resections or biopsies is cultured, whereas the tumor's architecture and its microenvironment are maintained. In addition, therapy-induced changes upon ex vivo immunotherapy treatment can be profiled. To assess whether IL-2 treatment had an additive effect to CTLA4 + PD1 blockade, we profiled the ex vivo responses of PDTFs from nine human tumor resections that included melanoma (MEL), non–small cell lung cancer (LU), renal cell carcinoma (RE), and ovarian carcinoma (OV) (Fig. 2A and table S3). These PDTFs were treated for 48 hours with either the dual combination of anti-CTLA4 + anti-PD1 or the triple combination therapy of anti-CTLA4 + anti-PD1 + IL-2 (Fig. 2A). Untreated fragments were used as a control for each culture. We assessed first whether anti-CTLA4 + anti-PD1 ± IL-2 had an impact on T cell activation by quantifying the expression of the activation markers OX40 and CD137 on CD8+ T cells, FOXP3− CD4+ T cells, and FOXP3+ CD4+ T cells (Fig. 2, B and C). Although dual checkpoint blockade infrequently induced activation of CD8+ T cells in PDTFs as compared with untreated tumor fragments, there was no notable effect on both FOXP3− and FOXP3+ CD4+ T cells. In contrast, the triple combination therapy induced activation of all three subsets and had the largest effect on FOXP3+ CD4+ T cells, in line with a previously described effect of IL-2 on the activation of regulatory T cells (Tregs) (*24–26*). Anti-CTLA4 + anti-PD1 + IL-2 also induced an increase in both the percentage and expression of FOXP3, which was not observed after anti-CTLA4 + anti-PD1 treatment (Fig. 2D). Thus, within the CD4+ T cell subset, the triple compared to dual combination therapy seemed to mainly cause a shift from FOXP3−OX40− to FOXP3+OX40+ cells (Fig. 2, E and F), suggesting that the triple combination therapy promotes the induction of activated FOXP3+ T cells.

To understand whether this increase in activated FOXP3+ T cells induced by the triple combination therapy related to an immune-activating or immunosuppressive response, we next examined 11 cytokines and 13 chemokines secreted by the PDTFs in an extended cohort of 16 tumors during steady state in untreated control cultures and in response to dual or triple combination immunotherapy (Figs. 2A and 3 and table S3). We first performed unsupervised hierarchical clustering of the cytokines and chemokines produced by PDTFs treated with dual checkpoint blockade compared with untreated PDTFs to identify ex vivo responders to CTLA4 + PD1 blockade. We found that the dual combination therapy induced changes in cytokine and chemokine secretion patterns in 4 of 16 (25%) tumors that we defined as anti-CTLA4 + anti-PD1 responders, whereas 12 of 16 (75%) of the tumors displayed only minor treatment-induced changes (anti-CTLA4 + anti-PD1 nonresponder) (Fig. 3A and fig. S2A). Next, we assessed responses to the triple combination–treated therapy condition within these two groups. The triple combination therapy converted 7 of 12 (58%) of the tumors that were anti-CTLA4 + anti-PD1 nonresponder into responder (anti-CTLA4 + anti-PD1 + IL-2 responder) (Fig. 3B and fig. S2B). In the anti-CTLA4 + anti-PD1 responder group, addition of IL-2 did not increase cytokine and chemokine secretion further (Fig. 3B and fig. S2B). Despite the induction of activated FOXP3+ T cells by the triple combination therapy, which may potentially include Tregs (Fig. 2, E and F), the induced immunological response was not suppressive but led to an increased IFN-γ and tumor necrosis factor–α (TNFα) secretion (Fig. 3, A and B). Overall, the response pattern induced by the triple combination therapy was comparable to the response elicited by the dual combination therapy (Fig. 3C).
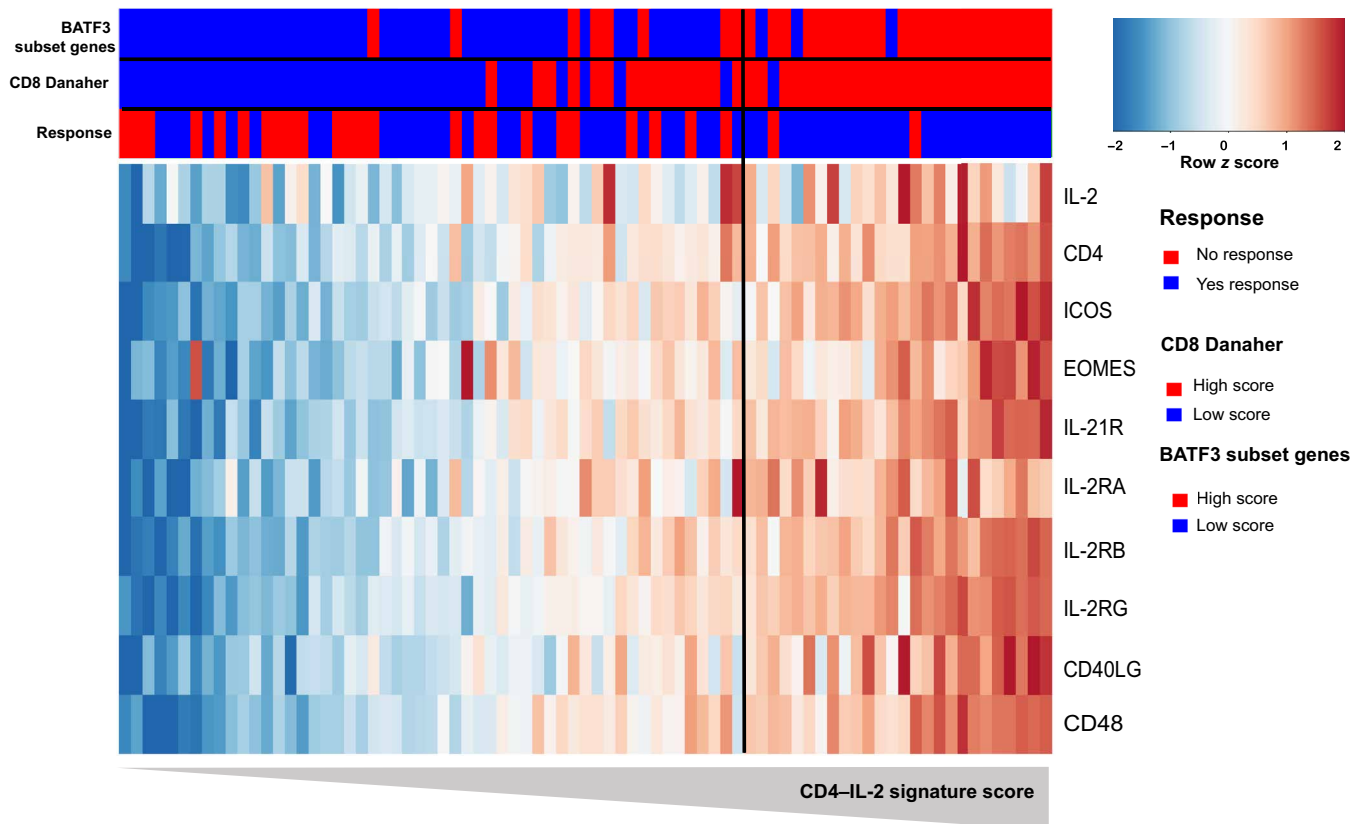
Kaptein *et al.*, *Sci. Transl. Med.* **14**, eabj9779 (2022)   27 April 2022

2 of 15

Fig. 1. A CD4/IL-2 gene signature is associated with response to neoadjuvant ipilimumab + nivolumab. Nanostring data of pretreatment lymph node tumor biopsies of patients with melanoma treated with neoadjuvant ipilimumab + nivolumab in the PRADO study (n = 79). The heatmap of the CD4/IL-2 gene signature is ordered according to the average expression of the CD4/IL-2 gene signature per patient. Each column displays one patient (blue: pathologic response, dark red: no pathologic response, blue: low BATF3/CD8 signature score, and light red: high BATF3/CD8 signature score). The scores of the BATF3/CD8 signatures were calculated on the basis of the average z score of *IRF8*, *THBD*, *XCR1* and *CD8A*, and *CD8B*, respectively. The optimal high-low cutoff was determined by the sROC curves (*56*) for each signature individually using both PRADO and OpACIN-neo patient data (n = 143). The rows in the heatmap represent the z score of the normalized gene expressions. Positive values (red) imply higher gene expression, and negative values (blue) indicate lower gene expression. The threshold to define a high CD4/IL-2 score is indicated by the black vertical line.

Although the nonresponding tumors showed a trend toward lower immune infiltration, particularly when compared with anti-CTLA4 + anti-PD1 + IL-2 responders (P = 0.09), the composition of the infiltrate showed no significant differences between the groups (Fig. 3D and fig. S3, A and B).

Addition of IL-2 to neoadjuvant anti-CTLA4 + anti-PD1 cures tumor-bearing mice

To confirm our ex vivo findings in an in vivo setting, we next tested the addition of IL-2 to dual checkpoint inhibition using the spontaneously metastatic triple-negative breast cancer model 4T1.2 (*3*). After 4T1.2 tumor inoculation in the mammary fat pad and before extensive primary tumor growth, mice develop extensive metastases in the lungs and other organs (*3*). Previously, we have demonstrated in our neoadjuvant 4T1.2 tumor model that the early expansion of peripheral tumor-specific CD8+ T cells after neoadjuvant immunotherapy strongly correlated with long-term survival (*3*). Therefore, we now investigated how the addition of IL-2 affected the efficacy of neoadjuvant anti-CTLA4 + anti-PD1 (Fig. 4). Groups of mice were treated with the indicated therapy on days 8 and 10 after 4T1.2 mammary fat pad inoculation, followed by surgery on day 13 (Fig. 4A).

Overall, the triple combination therapy (5/7) compared to the dual combination therapy (3/10) cured a greater proportion of mice, although all treatments either prolonged survival after surgery or conferred long-term survival benefits compared with the control immunoglobulin (Ig)–treated group (Fig. 4A). 4T1.2, like many murine cancer cell lines, express the envelope glycoprotein (gp70) encoded by the murine leukemia virus (MuLV). Gp70 in the tumor only functions as a neoantigen to induce tumor-specific T cell responses (*27*). This allowed us to address whether the addition of IL-2 to CTLA4 + PD1 blockade resulted in a stronger expansion and activation of tumor-specific CD8+ T cells. From the experiment shown in Fig. 4A, we performed longitudinal analysis of gp70 tetramer–specific CD8+ T cells in the peripheral blood of tumor-bearing mice before and after treatment with either the dual combination therapy of anti-CTLA4 + anti-PD1, triple combination therapy of anti-CTLA4 + anti-PD1 + IL-2, IL-2 alone, or control Ig (cIg) alone (Fig. 4B and fig. S4). We observed the greatest increase in gp70-specific T cells in mice treated with the triple combination therapy compared with either the dual checkpoint inhibitor combination therapy, IL-2 alone, or cIg alone (Fig. 4B). Furthermore, the majority of gp70-specific T cells in the triple combination

Kaptein *et al.*, *Sci. Transl. Med.* **14**, eabj9779 (2022)   27 April 2022

3 of 15

Fig. 2. Activation of distinct T cell subsets upon addition of IL-2 to ex vivo CTLA4 + PD1 blockade in resected tumors derived from patients with cancer. (**A**) Experimental overview of the PDTF platform. (**B** and **C**) Expression of T cell activation markers in unstimulated, anti(α)CTLA4 + αPD1− and αCTLA4 + αPD1 + IL-2–treated CD8$^+$ T cells, and CD4$^+$FOXP3$^−$ and FOXP3$^+$ T cells measured by flow cytometry ($n = 9$ tumors). Box plot with mean and range is shown. (**D**) Flow plots showing FOXP3 expression and fold change of FOXP3 percentage and geometric mean fluorescence intensity (GMFI) in αCTLA4 + αPD1− and αCTLA4 + αPD1 + IL-2–treated CD4$^+$ T cells compared with untreated CD4$^+$ T cells. Shown are means ± SEM. The distinct symbols in (C) and (D) indicate different tumor types. (**E** and **F**) Expression and quantification of OX40 and FOXP3 in untreated, αCTLA4 + αPD1−, and αCTLA4 + αPD1 + IL-2–treated CD4$^+$ T cells. Significant differences between groups were determined by Kruskal-Wallis test (C) or Mann-Whitney test (D). **$P < 0.01$ and ****$P < 0.0001$.
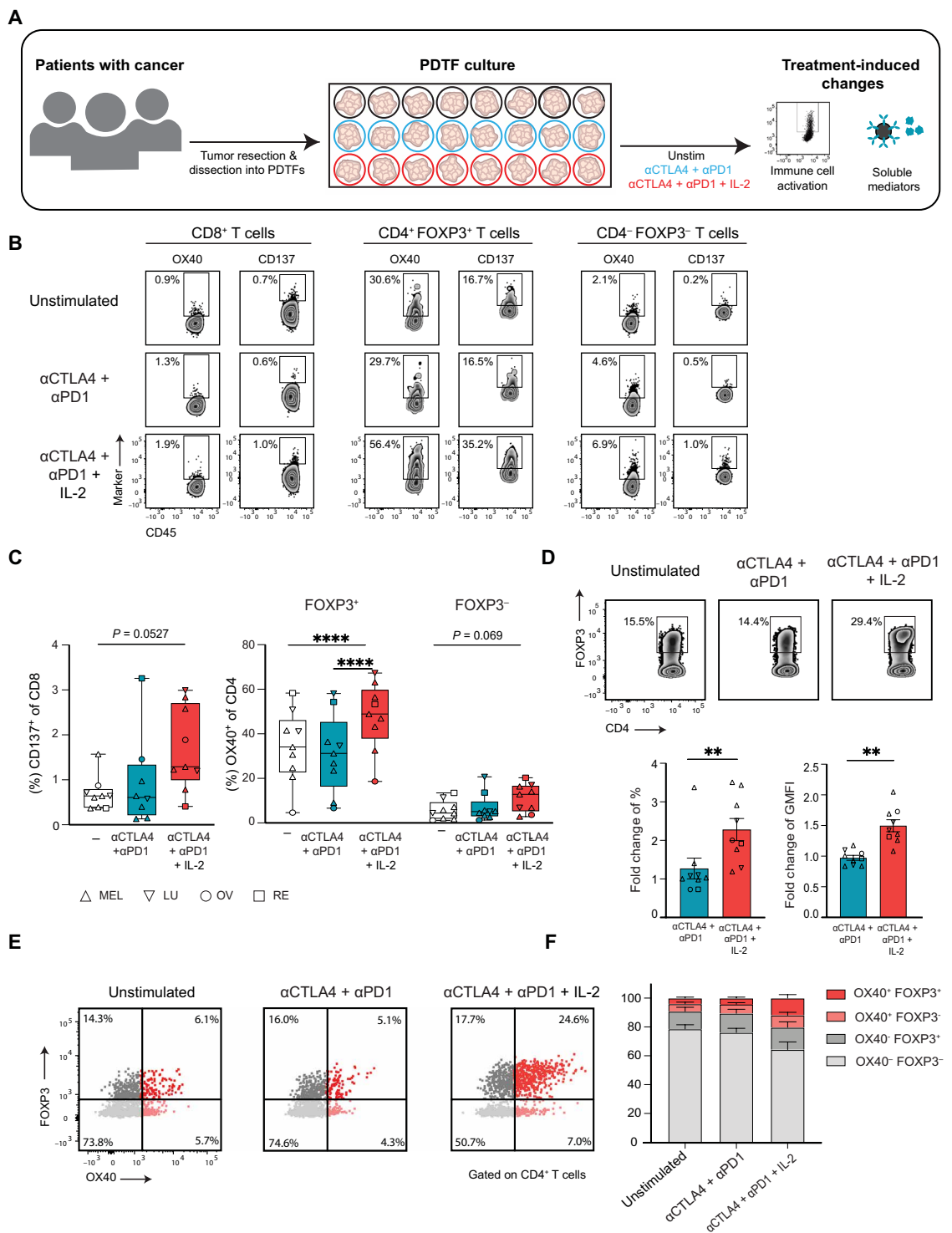
therapy–treated group expressed CX3CR1 (fig. S5A) and KLRG1 (fig. S5B), suggesting a terminally differentiated T cell effector phenotype (*28, 29*). In addition, we observed an increase in non-gp70 tetramer reactive CD8$^+$ T cells expressing this effector phenotype in the triple combination therapy compared with the dual combination therapy–treated mice early after treatment, indicating a possible broadening of the tumor-specific T cell repertoire (fig. S5, C and D).

We next determined which innate and adaptive immune cells were important for the efficacy of neoadjuvant anti-CTLA4 + anti-PD1 + IL-2 (Fig. 4, C to F). In a similar experimental setup as Fig. 4A, 4T1.2 tumor–bearing BATF3-deficient mice, which lack cross-presenting CD103$^+$CD8α$^+$ DC, were treated with neoadjuvant triple combination immunotherapy. These mice displayed a complete loss of long-term survivors compared with similar groups

Kaptein *et al.*, *Sci. Transl. Med.* **14**, eabj9779 (2022)   27 April 2022

4 of 15
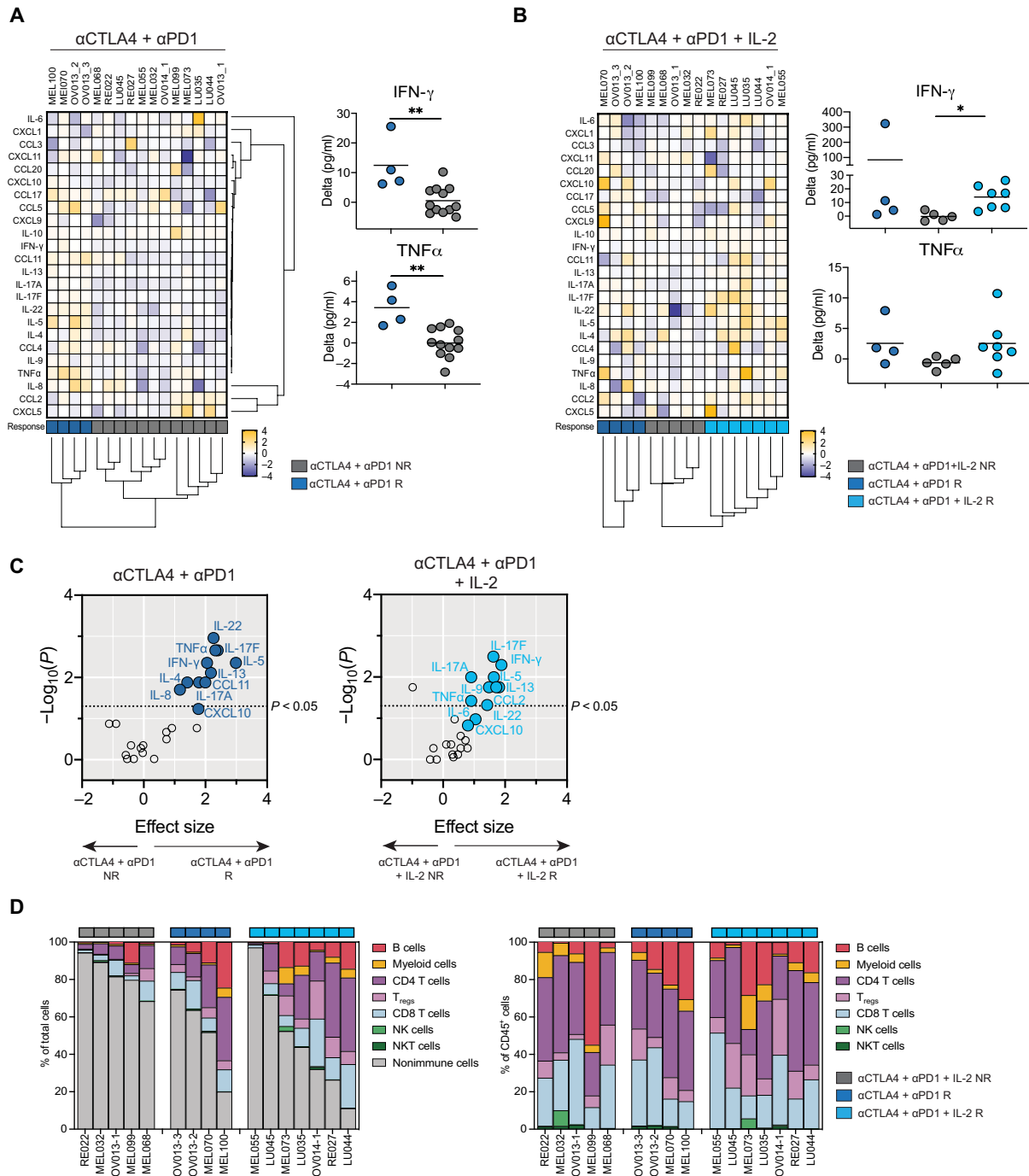
Fig. 3. Addition of IL-2 induces immunological responses in human ex vivo tumors that are nonresponsive to anti-CTLA4 + anti-PD1 therapy. (**A**) Heatmap displaying the normalized delta values between the untreated and anti-CTLA + anti-PD1 conditions for each parameter (11 cytokines and 13 chemokines, $n = 16$ tumors) (left). Unsupervised clustering identified two groups of tumors: anti(α)CTLA4 + αPD1 responders (R) and αCTLA4 + αPD1 nonresponders (NR). Changes in IFN-γ and TNFα secretion within the two response groups are displayed in the right panel. Shown are the delta values between the anti-CTLA4 + anti-PD1–treated minus the untreated condition; each dot represents a single tumor. The line indicates the mean. (**B**) Heatmap showing the normalized delta values between the untreated and αCTLA4 + αPD1 + IL-2–treated conditions for the same parameters as in (A, left). Supervised clustering identified two subgroups within the αCTLA4 + αPD1 NR group: αCTLA4 + αPD1 + IL-2 R and αCTLA4 + αPD1 + IL-2 NR tumors. Changes in IFN-γ and TNFα secretion within the two response groups are displayed in the right panel. Shown are the delta values between the anti-CTLA4 + anti-PD1 + IL-2–treated minus the untreated condition; each dot represents a single tumor. The line indicates the mean. (**C**) Correlation between effect sizes (calculated as Hedge's g) and P values of normalized changes for all parameters assessed in the αCTLA4 + αPD1 and αCTLA4 + αPD1 + IL-2 treatment groups. (**D**) Quantification of immune cell subsets assessed by flow cytometry within total live cells (left) and total CD45$^+$ immune cells (right). Significant differences between groups were determined by Mann-Whitney test (A) or Kruskal-Wallis test (B). *$P < 0.05$ and **$P < 0.01$. NK, natural killer cells; NKT, natural killer T cells.
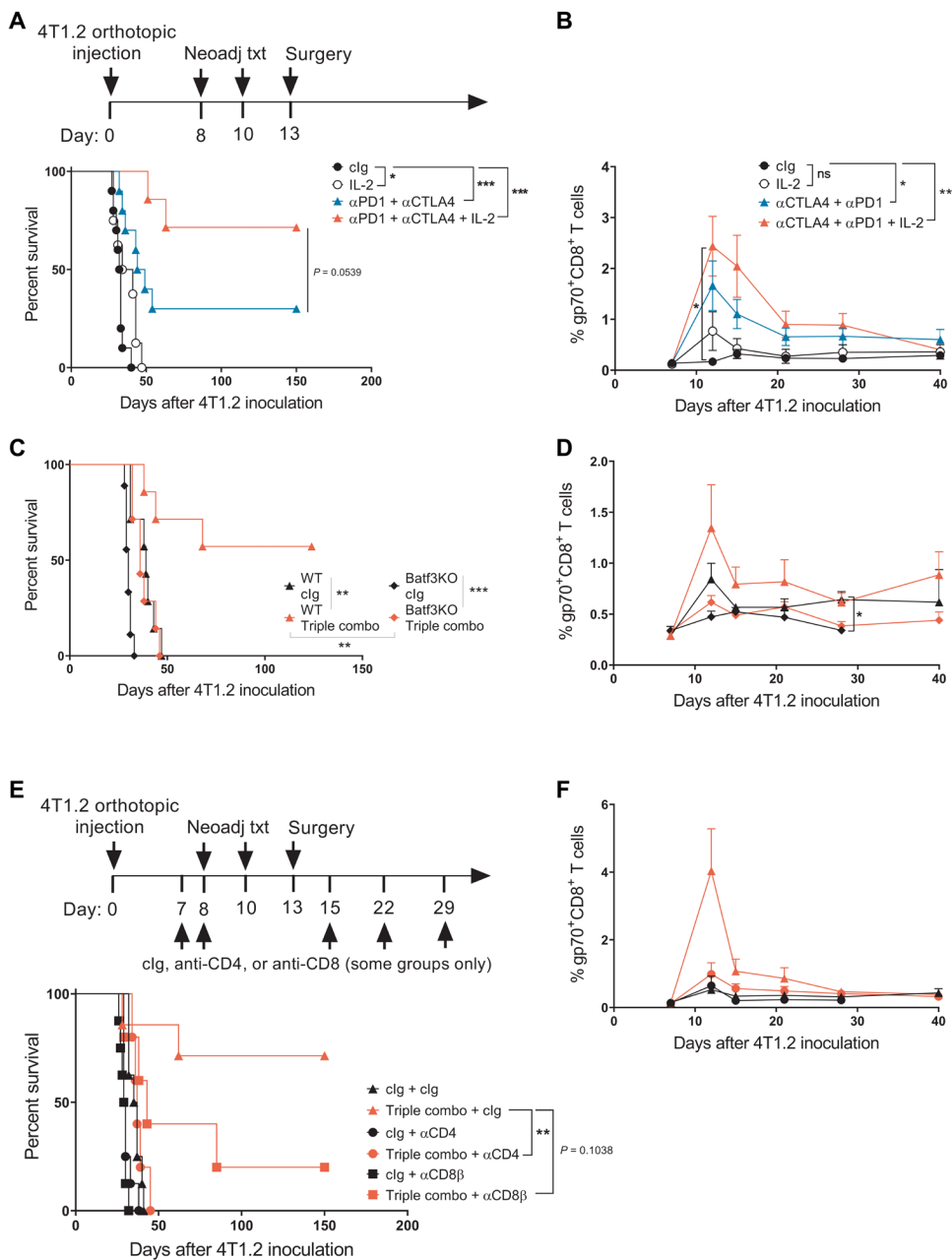
Fig. 4. Addition of IL-2 to neoadjuvant anti-CTLA4 + anti-PD1 eradicates metastatic disease via improved expansion of tumor-specific CD8+ T cells in 4T1.2 tumor–bearing mice. (A, B, E, and F) Groups of BALB/c wild-type (WT) or (C and D) Batf3KO mice were injected in the mammary fat pad with 4T1.2 tumor cells and treated intraperitoneally on days 8 and 10 with the indicated combination of anti-CTLA4, anti-PD1, IL-2, or cIg, followed by resection of the primary tumor on day 13 as indicated. (E and F) In addition, some groups of mice were treated with cIg, anti-CD4, or anti-CD8β on days 7, 8, 15, 22, and 29. (A, C, and E) Kaplan-Meier curves for overall survival of each group are shown. (B, D, and F) Proportion of gp70 tetramer+ CD8+ T cells in the blood of treated mice at the indicated time points (mean + SEM). (A to F) All experiments were double blinded and performed once (n = 5 to 10 per group). Significant differences between the indicated groups were determined by (A, C, and E) log-rank test or (B, D, and F) mixed effects analysis with Tukey's multiple comparisons test. *P < 0.05, **P < 0.01, ***P < 0.001, and ****P < 0.0001. Triple combo: anti-CTLA4 + anti-PD1 + IL-2.

neoadjuvant triple combination immunotherapy was also demonstrated (Fig. 4, E and F) by performing T cell–specific depletions. CD4+ T cell depletion in 4T1.2 tumor–bearing mice starting 1 day before commencement of neoadjuvant triple combination immunotherapy resulted in the complete loss of long-term survivors (0/5, 0%) compared with the cIg-treated triple neoadjuvant immunotherapy group (5/7, 71%) (**P < 0.01) (Fig. 4E). This correlated with a lack of gp70-specific T cell expansion in the CD4+ T cell–depleted group that was treated with the triple combination therapy (Fig. 4F). Similarly, CD8+ T cell depletion before neoadjuvant anti-CTLA4 + anti-PD1 + IL-2 treatment reduced the proportion of long-term survivors compared with the triple combination therapy–treated group, although this abrogation of survival was not as notable as that seen with CD4+ T cell depletion.

We next evaluated the importance of CD4+ T cells in the priming of a natural CD8+ T cell response before neoadjuvant immunotherapy or in the response against metastases after both surgery and treatment. We therefore set up a similar experiment as in Fig. 4E, where we depleted CD4+ T cells at two different time points in neoadjuvant triple combination–treated mice (fig. S6). In one group, CD4+ T cell depletion began at day −1 before tumor inoculation (triple combo + anti-CD4 d-1), and in the other group, depletion occurred 1 day after surgery at day 14 (triple combo + anti-CD4 d14). There was no significant difference in survival between the group of mice in the triple combo + anti-CD4 d14 group and the non–CD4-depleted group [(5/11 (45%) versus 7/12 (58%), respectively)] (fig. S6A). This suggests that the CD4+ T cells helper or direct-killing functions may not be as critical to survival after primary tumor removal. In contrast, the triple combo + anti-CD4 d-1 group had significantly reduced survival compared with the non–CD4-depleted group (***P < 0.001) (fig. S6A), similar to what we observed when depleting CD4+ T cells at day 7 before neoadjuvant immunotherapy (Fig. 4E). In this experiment, we also measured longitudinally the proportion of gp70-specific CD8+ T cells in the blood, and we observed that only the mice from triple combo + anti-CD4 d-1 group failed to expand tumor-specific CD8+ T cells in comparison to other

of treated tumor-bearing WT mice (Fig. 4C). This was supported by the lack of gp70-specific T cell expansion in the treated BATF3-deficient compared with WT mice (Fig. 4D). Furthermore, a requirement for both CD4+ and CD8+ T cells for the efficacy of

triple combo–treated groups (fig. S6B). Overall, these data and Fig. 4E suggest CD4^{+} T cells are critical for priming of natural and treatment-induced CD8^{+} T cell immunity against 4T1.2 tumors and for helping in the expansion of gp70 tumor–specific CD8^{+} T cells early after neoadjuvant immunotherapy. However, they may not be as important after resection of the primary tumor.

To further investigate the mechanism by which IL-2 improved the efficacy of neoadjuvant anti-CTLA4 + anti-PD1, we set up an experiment similar to Fig. 4, where neoadjuvant triple or double combination immunotherapy was compared and peripheral blood was collected 2 days after the final treatment (Fig. 5). At the time point when the primary tumor is normally resected (day 13), we culled the mice; collected the primary tumor, spleen, and draining lymph node; and generated single-cell suspensions for flow cytometry analyses (Fig. 5). As we previously observed in Fig. 4B, triple combination immunotherapy resulted in the greatest expansion of gp70-specific T cells in the peripheral blood compared with dual combination immunotherapy or IL-2 alone (**$P < 0.01$) (fig. S7). We observed that the triple, compared to double combination immunotherapy–treated group had an increased proportion of gp70^{+} CD8^{+} T cells, gp70^{neg} CD8^{+} T cells, and CD4^{+} T conventional (Tconv) cells that expressed intracellular IFN-γ, TNF, and IL-2, which are typical proinflammatory cytokines (Fig. 5, B to I, and fig. S8). A similar increase in proinflammatory cytokine polyfunctionality was also observed in CD4^{+} FOXP3^{+} cells, which are considered to be Tregs (Fig. 5, F to I). Specifically, the triple combination immunotherapy compared with dual combination immunotherapy improved the quality of the different T cell subsets as measured by an increase in the expression of IFN-γ, IL-2, and TNF (fig. S9). To determine whether the addition of IL-2 to neoadjuvant anti-CTLA4 + anti-PD1 treatment changed the phenotype of CD4^{+} Tconv and Tregs, we performed flow cytometry analysis for a number of surface markers of Tconv and Tregs from day 13 resected tumors (the time point we performed previous analyses for Fig. 5) (fig. S10). The markers we assessed included various costimulatory receptors (CD226, ICOS, CD137, and OX40) or inhibitory receptors (CD39, CTLA4, NRP1, PD1, and TIGIT). Overall, the changes observed in the CD4^{+} Tconv and Treg phenotype were mainly due to neoadjuvant anti-CTLA4 + anti-PD1 therapy, because the same trends were observed in both dual combination– and triple combination–treated groups (fig. S10). In conclusion, the addition of IL-2 in the triple combination therapy works mainly by increasing the production of TH1 cytokines (Fig. 5) rather than changing costimulatory or inhibitory receptor expression on CD4^{+} T cells.

To determine whether the addition of IL-2 to the dual combination immunotherapy improved proliferation, we also measured Ki67 staining on these T cell subsets. Overall, we observed an increase in the proliferation of all T cell subsets in the triple combination or dual combination immunotherapy groups compared with the cIg-treated group in tumor, draining lymph node, and spleen (fig. S11). However, there were no significant differences between triple combination– or dual combination immunotherapy–treated groups. We also observed no difference in the T cell subset proportion in tumor-infiltrating leukocytes after the triple combination immunotherapy, dual combination immunotherapy, or cIg treatment (fig. S12A). In the literature, it was reported that improved antitumor immunity in mouse models of cancer was associated with an increase in effector T cell–to–Treg ratio (30). However, we observed no significant changes between the effector T cell–to–Treg ratio in

immunotherapy-treated and cIg-treated groups (fig. S12B). Overall, our preclinical data demonstrated that the triple combination therapy of neoadjuvant anti-CTLA4 + anti-PD1 + IL-2 compared with dual CTLA4 + PD1 blockade cured a high proportion of mice with metastatic disease. This was due to improved expansion of tumor-specific CD8^{+} T cells, increased production of TH1 cytokines by total CD8^{+} and CD4^{+} T cells, and also by FOXP3^{+} CD4^{+} T cells.

Addition of IL-2 to CTLA4 + PD1 blockade induces immune responses in pretreatment biopsies from patients with melanoma resistant to neoadjuvant ipilimumab + nivolumab

To assess whether the addition of IL-2 also induced immunological responses in CTLA4 + PD1 blockade–resistant tumors in the neoadjuvant clinical setting, we treated baseline biopsies from 16 patients with melanoma enrolled in the PRADO cohort of the OpACIN-neo trial (NCT02977052) with anti-CTLA4 + anti-PD1 + IL-2 ex vivo. We were able to collect eight pretreatment samples from patients who achieved a pathological response upon neoadjuvant ipilimumab + nivolumab (defined as pCR, near pCR, or pPR; "PRADO responder") and eight pNR samples ("PRADO nonresponder") (table S4). Because of the small size of the baseline biopsies ($1\times$ 12 to 14 g), assessment of responses was limited to the detection of soluble parameters in the unstimulated and anti-CTLA4 + anti-PD1 + IL-2–treated conditions (Fig. 6A). As the smaller number of PDTFs per condition may induce more noise in the data, we aimed to identify the most relevant parameters for response by performing AUC analysis of each cytokine and chemokine secreted by the PDTFs from the resection cohort described in Fig. 3. This revealed that the separation of anti-CTLA4 + anti-PD1 and anti-CTLA4 + anti-PD1 + IL-2–responding and –nonresponding resected tumors was mostly driven by an increase in a subset of parameters, including IFN-γ, IL-22, and CXCL10. This information was used to establish a response score based on the seven most discriminative parameters (Fig. 6B and fig. S13) to facilitate the classification of the biopsies as either responder or nonresponder. Using this response score, we observed that anti-CTLA4 + anti-PD1 + IL-2 induced an immunological response in seven of eight (87.5%) tumor biopsies from PRADO pathologic responders (Fig. 6, C and D), in line with the data obtained from tumor resections showing that tumors responding to dual checkpoint blockade also respond to the triple combination treatment (Fig. 3, A and B). Within the PRADO pathologic nonresponder group, treatment with the triple combination induced immunological responses in five of eight (62.5%) tumor biopsies (Fig. 6, C and D, and fig. S14A). For 12 of 16 biopsies, for which sufficient material was available, we also measured the release of six cytotoxic molecules (granulysin, granzyme A and B, perforin, sFas, and sFasL) after anti-CTLA4 + anti-PD1 + IL-2 treatment. The triple combination therapy increased the release of cytotoxic mediators in anti-CTLA4 + anti-PD1 and anti-CTLA4 + anti-PD1 + IL-2 responders, whereas no changes were observed in nonresponding tumors (Fig. 6E and fig. S14B). Overall, these results suggest that the addition of IL-2 to CTLA4 + PD1 blockade may induce immune activation in tumors resistant to neoadjuvant anti-CTLA4 + anti-PD1 that is comparable to those observed for responders to dual checkpoint blockade.

DISCUSSION
Neoadjuvant checkpoint inhibition, and especially the combination of CTLA4 + PD1 blockade, is currently the most promising therapeutic
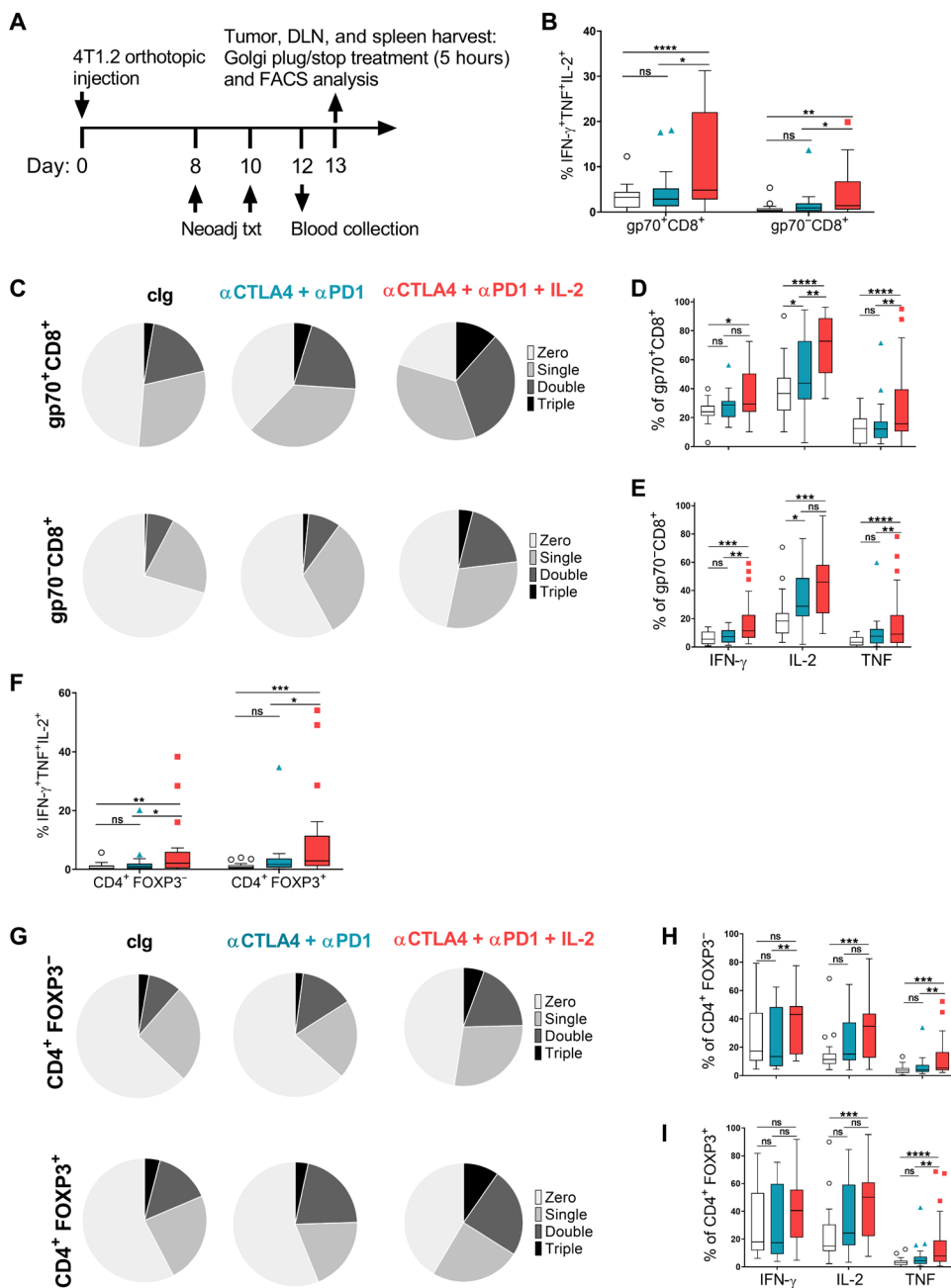
Fig. 5. Addition of IL-2 to neoadjuvant anti-CTLA4 + anti-PD1 improves both CD8+ and CD4+ T cell cytokine polyfunctionality in 4T1.2 tumor–bearing mice. (A to I) Groups of BALB/c WT mice were injected in the mammary fat pad with 4T1.2 tumor cells and treated intraperitoneally on days 8 and 10 with the indicated combination of anti-CTLA4, anti-PD1, IL-2, or cIg. On day 12, peripheral blood was collected from all groups of mice (B), and at day 13, tumors (C to I) were harvested and single-cell suspensions generated for flow cytometry analysis. Gating on live CD45.2+ cells of leukocyte morphology, the proportion of the indicated (B) gp70 tetramer+/− CD8+ T cells or (F) CD4+ FOXP3− (T_{conv}) or CD4+ FOXP3+ (T_{reg}) cells coexpressing intracellular IFN-γ, TNF, and IL-2. Box plot with Tukey's whiskers of (C) gp70 tetramer+/− CD8+ T cells or (G) CD4+ Tconv or T_{regs} expressing zero, one, two, or three cytokines (of IFN-γ, TNF, and IL-2) or (D, E, H, and I) the individual cytokines. Data pooled from three independent experiments that were performed and analyzed double blinded (n = 15 to 23 per group). Statistical comparisons between groups were performed by two-way ANOVA with Tukey's multiple comparisons test, *P < 0.05, **P < 0.01, ***P < 0.001, and ****P < 0.0001. ns, not significant.

option for macroscopic stage III melanoma. Very high pRR of 71 to 80%, long-term RFS rates of 80%, and overall survival of 90% have been observed in neoadjuvant checkpoint inhibitor–treated patients with melanoma (6–8, 10). This is in contrast to patients receiving surgery alone who are expected to have an RFS of 30% and 5-year overall survival in the range of 50% (31–33). Even though the randomized registration trial comparing neoadjuvant ipilimumab + nivolumab versus adjuvant nivolumab (NADINA) has just started (end of 2021), two major questions remain: how to identify patients who will benefit from the current therapeutic options, and what alternative neoadjuvant combination therapy could be offered to patients with unfavorable tumor characteristics, who are unlikely to respond to neoadjuvant ipilimumab + nivolumab. We have recently shown that a high-baseline IFN-γ signature and high TMB were associated with 100% pathologic response and a subsequent excellent RFS rate. In addition, having only one of the two favorable parameters was still associated with about 90% chance of response. In contrast, only 39% of patients lacking both factors responded (10). Of note, the feasibility of applying such IFN-γ–signature algorithms prospectively in trials to personalize neoadjuvant immunotherapy has recently been shown (34).

In search for rational treatment combinations for patients with melanoma who are unlikely to respond to neoadjuvant ipilimumab + nivolumab, we performed extended human RNA signature analyses. In addition to the previously described IFN-γ, T cell, and BATF3 signatures (4, 12), we here found and confirmed in an independent cohort, a newly designed CD4/IL-2 signature that correlated with outcome upon neoadjuvant ipilimumab + nivolumab. In a previous study, Raeber et al., (16) used an IL-2 signature derived from human T cells stimulated with IL-2 (35) to analyze The Cancer Genome Atlas data of a cohort of human skin cutaneous melanoma mostly derived from advanced cancers, comprising 20% primary cutaneous melanomas and 80% metastases (36). They found that patients whose tumors displayed a high IL-2 signature had prolonged survival (16). In contrast, our CD4/IL-2 signature derives from baseline
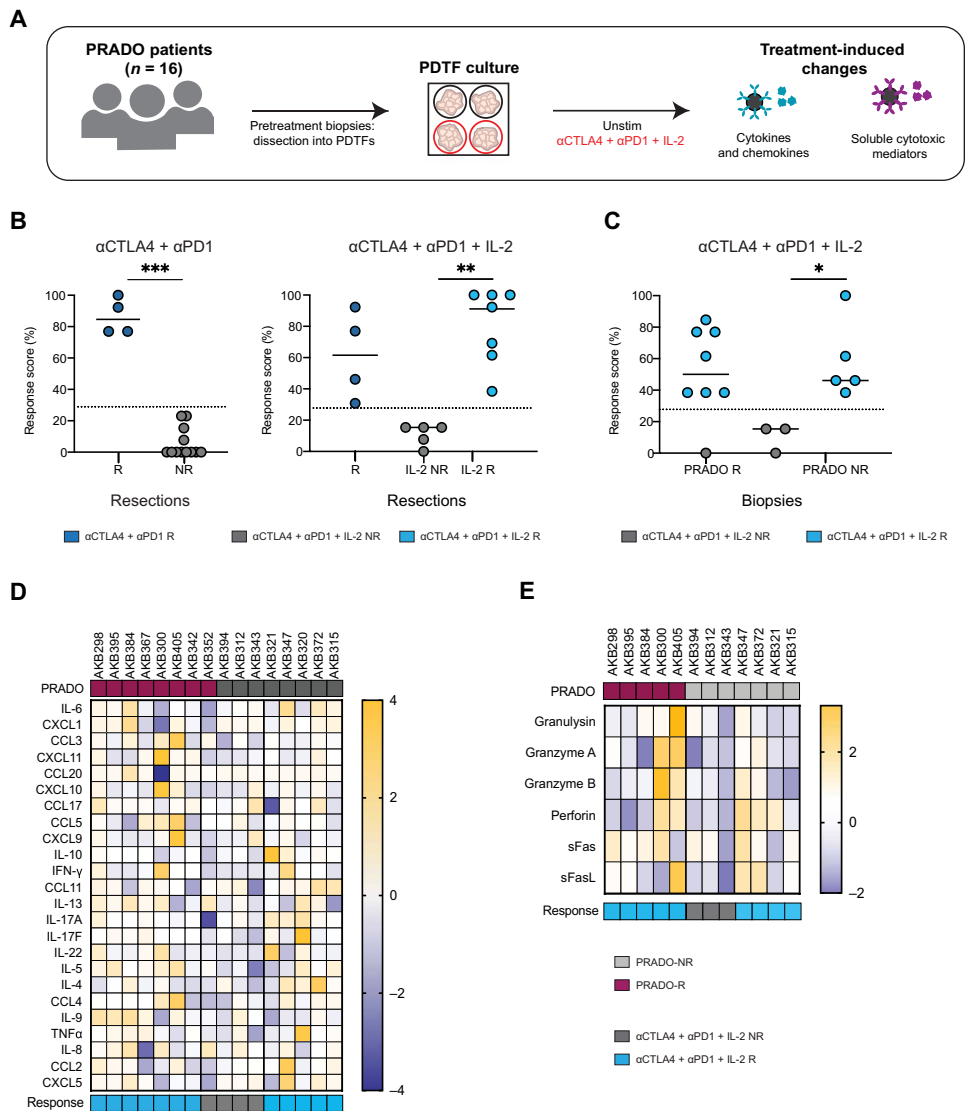
Fig. 6. Addition of IL-2 to CTLA4 + PD1 blockade ex vivo induces immunological responses in pretreatment biopsies of patients with melanoma resistant to dual checkpoint blockade. (**A**) Schematic overview of the experimental outline using human tumor biopsies. (**B**) Response scores based on the parameters (IL-5, IL-17A, IL-17F, IL-22, IFN-γ, TNFα, and CXCL10) that best predict response for the anti-CTLA4 + anti-PD1 and anti-CTLA4 + anti-PD1 + IL-2 treatment groups derived from the 16 resected tumors from Fig. 3. (**C**) Response scores for each pretreatment melanoma tumor biopsy (n = 16) collected from the PRADO trial, identifying three groups of tumors: αCTLA4 + αPD1 + IL-2 R (within PRADO-R), αCTLA4 + αPD1 + IL-2 NR, and αCTLA4 + αPD1 + IL-2 R (both within PRADO-NR). The lines in (B) and (C) indicate the mean. The dashed line indicates the cutoff of the response score. (**D**) Heatmap displaying the normalized delta values between the untreated and αCTLA4 + αPD1 + IL-2–treated condition for each parameter (11 cytokines and 13 chemokines, n = 16 pretreatment tumor biopsies). The two groups were separated on the basis of clinical response (pR versus pNR) to αCTLA4 + αPD1. (**E**) Heatmap displaying the normalized delta values between the untreated and αCTLA4 + αPD1 + IL-2–treated condition for six cytotoxic mediators (n = 12 pretreatment tumor biopsies from the PRADO cohort). Significant differences between groups were determined by Mann-Whitney test (B, left) or Kruskal-Wallis test (B, right, and C). *P < 0.05, **P < 0.01, and ***P < 0.001.

pretreatment tumor biopsies of patients with less-advanced stage III melanoma. In addition to predicting patients who will respond to neoadjuvant ipilimumab + nivolumab, it will also be interesting to determine whether our CD4/IL-2 signature has prognostic or predictive value for patients with late-stage melanoma. Although the addition of IL-2 has been shown to (i) improve efficacy of checkpoint inhibition in large tumor burden mouse models and (ii) decrease metastatic burden in 4T1 tumor–bearing mice and (iii) in late-stage disease of a patient in combination with adoptive tumor-infiltrating lymphocytes transfer (17, 18, 37), the efficacy of this combination has not been explored in any neoadjuvant setting. The strong predictive capability of the CD4/IL-2 signature led us therefore to analyze the addition of IL-2 to anti-CTLA4 + anti-PD1 in a mouse tumor model of neoadjuvant immunotherapy and ex vivo in human tumor fragments. The triple combination immunotherapy compared with the dual combination immunotherapy improved the activation and effector function of both CD8^{+} and CD4^{+} tumor-infiltrating lymphocytes as measured by the up-regulation of T cell activation markers and the coexpression of IFN-γ, TNF, and IL-2 in both human and murine settings. Although we previously demonstrated that the efficacy of neoadjuvant anti-PD1 + anti-CD137 was dependent on the presence of CD8^{+} T cells and partially dependent on CD4^{+} T cells (3), herein, neoadjuvant anti-CTLA4 + anti-PD1 + IL-2 was fully dependent on the presence of CD4^{+} T cells and partially dependent on CD8^{+} T cells. This may be due to the type of combination immunotherapy that was assessed in the current compared with our previous study. Furthermore, our data also suggested that these CD4^{+} T cells were critical for the expansion of tumor-specific CD8^{+} T cells because CD4 depletion before or early during neoadjuvant triple combination therapy completely abrogated their expansion in the blood, which was not the case when CD4^{+} T cells were depleted after surgery. Potentially, these CD4^{+} T cells may contribute to help CD8^{+} T cell responses as previously reported (38), given the significantly increased proportion of CD4^{+}FOXP3^{−} helper T cells that produced IL-2 after the triple combination immunotherapy compared with the dual combination immunotherapy. It is important to note that this effect may not be restricted to IL-2 but may also be achieved by combining ICI with other cytokines that can overcome the lack of CD4 help and support CD8^{+} T cell activation.

In addition to its role in stimulating conventional T cells, IL-2 has been shown to promote the induction, survival, and function of T_regs (24–26). In our study, the overall effects of adding IL-2 to CTLA4 + PD1 blockade were positive as observed by the increased

proportion of effector CD8$^+$ and CD4$^+$ T cells with cytokine poly-functionality (IFN-γ, TNFα, and IL-2) and T cell proliferation in our mouse model. Similarly, in our ex vivo PDTF cultures, the addition of IL-2 converted a proportion of anti-CTLA4 + anti-PD1 immunological nonresponders into responders as measured by the induction of a proinflammatory response including increased IFN-γ and TNFα secretion. This response was induced despite the expansion of activated CD4$^+$FOXP3$^+$ T cells by the triple combination. Whether these CD4$^+$FOXP3$^+$ T cells represent true T$_{regs}$ with suppressive function or CD4$^+$ effector T cells that acquire FOXP3 expression during activation (39, 40) will require further investigation. In mice, FOXP3 expression appears to be sufficient to define CD4$^+$ T$_{regs}$ (41), but our preclinical data suggested that tumor-infiltrating T$_{regs}$ from neoadjuvant anti-CTLA4 + anti-PD1 + IL-2–treated mice also displayed a strong T$_H$1 cytokine profile. T$_{regs}$ producing IFN-γ despite retaining FOXP3 expression have previously been described to have a "fragile" phenotype characterized by having reduced suppressive activity due to loss of Nrp1 (42). CD122-selective IL-2 complexes were reported to reduce immuno-suppression, promote T$_{reg}$ fragility, and sensitize tumor response to programmed death-ligand 1 (PD-L1) blockade (43). However, it is unlikely that this phenotype is the reason for the improved efficacy of neoadjuvant anti-CTLA4 + anti-PD1 + IL-2 as these mice showed an increase in the proportion of T$_{regs}$ expressing Nrp1 compared with those that received cIg or IL-2. CTLA4 blockade in murine tumor models has recently been shown to promote functional destabilization of T$_{regs}$ in poorly glycolytic tumor microenvironments, which correlated with an improvement in CD8 effector function (44). Similarly, PD1 blockade has been described to increase IFN-γ expression in T$_{regs}$ (45). Overall, both our animal and human data support the notion that the addition of IL-2 to anti-CTLA4 + anti-PD1 affects antitumor immunity positively rather than negatively and can convert tumors from nonresponsive to responsive to CTLA4 + PD1 blockade.

To confirm our findings in a more relevant, thus neoadjuvant clinical setting, we assessed the effect of the triple combination immunotherapy in pretreatment biopsies of patients with stage III melanoma systemically treated with neoadjuvant ipilimumab + nivolumab. These experiments suggest that the triple combination of anti-CTLA4 + anti-PD1 + IL-2 can induce immunological responses in about 50% of melanoma lesions from patients who are resistant to dual immune checkpoint blockade, thus providing a rationale to test this combination clinically.

Our study has some limitations. Although it would have been useful to demonstrate our preclinical findings in additional mouse cancer models, we used the 4T1.2 tumor model because it best mimics the clinical setting of surgery and therapy of residual meta-static disease as observed in patients with cancer, where it will result generally in death of mice if not treated. In contrast, carcinogen-induced and genetically modified mouse models as well as most transplant models of cancer do not offer this opportunity. Few truly metastasize, and metastasis is generally minimal relative to primary tumor size with late resection becoming impractical and unethical. Next, although we demonstrated preclinically that the efficacy of neoadjuvant anti-CTLA4 + anti-PD1 + IL-2 required the presence of T$_H$1 cytokine–producing CD4$^+$ T cells, it is unclear whether those CD4$^+$ T cells are tumor reactive. More in-depth studies are required to understand the mechanisms by which CD4 T cells mediate anti-tumor efficacy in the neoadjuvant setting. Last, in our study, we

combined dual checkpoint blockade with systemic IL-2. Because systemic IL-2 can induce potential toxicities, such as capillary leak syndrome caused by IL-2's high affinity for CD25 (IL-2Rα), which is expressed on the pulmonary vasculature (46), alternative ways of application are necessary to avoid toxicity. One potential way to avoid toxicity would be to use intratumoral injection of IL-2 or the use of targeted IL-2 variants. Some examples include the CD25 mimobody that abolishes CD25 binding (47), as well as variants that target IL-2 to the tumor microenvironment (48) or to effector CD8 (49) or PD1-expressing T cells (50). Taking into consideration a likely higher adverse event rate, one may preferentially test this triple combination immunotherapy in a personalized manner in patients with unfavorable tumor characteristics such as low TMB, low CD4/IL-2, or low IFN-γ signature. Moreover, given that TMB analyses are laborious, time-consuming, and expensive, it will be important to compare their predictive value with our newly developed CD4/IL-2 signature, as the latter may help to identify suitable patients in an easier manner. Potentially, the predictive value of this signature can also be evaluated in other cancer types where neoadjuvant ipilimumab + nivolumab is currently being tested (51–53).

Overall, our study shows how the combination of signature-driven analyses and functional assessment of patient tumor samples ex vivo, together with mechanistic experiments in in vivo mouse models can be used to identify potential treatment strategies for neoadjuvant combination checkpoint–resistant melanoma. This study provides a rationale for testing the neoadjuvant combination of anti-CTLA4 + anti-PD1 + IL-2 in patients with melanoma with unfavorable tumor characteristics.

MATERIALS AND METHODS
Study design
This study was intended to examine whether additional IL-2 immunotherapy can overcome resistance to neoadjuvant anti-CTLA4 and anti-PD1 in patients with melanoma. In pretreatment biopsies from PRADO and OpACIN trials, we studied an IL-2 gene signature for its association with resistance to neoadjuvant immune checkpoint blockade. OpACIN, OpACIN-neo, and PRADO were open-label, phase 1b and II studies testing neoadjuvant ipilimumab + nivolumab in macroscopic stage III melanoma, which have been described before extensively (4, 7, 8). All baseline samples with sufficient material were included. No blinding was applied. No randomization took place (the PRADO cohort served as the exploratory cohort, whereas the OpACIN baseline samples served as the confirmatory cohort).

Ex vivo stimulation of PDTFs was used to assess whether impaired response in resistant patients can be reversed by the addition of IL-2. Tumors were selected on the basis of >10% immune cell infiltration. Randomization was not necessary because all treatment conditions could be directly compared within a tumor sample. Pretreatment biopsies from the PRADO study were selected on the basis of clinical treatment response and availability of material. Researchers performing the ex vivo experiments were blinded to the clinical outcome. Preclinical studies in neoadjuvant-treated mice helped to decipher the mechanism by which addition of IL-2 increased survival and induced a more potent antitumor immune response. In vivo mouse experiments were performed using BALB/c WT and BALB/c Batf3-deficient mice, which were bred and maintained at the QIMR Berghofer Medical Research Institute.

Kaptein *et al.*, *Sci. Transl. Med.* **14**, eabj9779 (2022)   27 April 2022

10 of 15

Female mice 8 weeks and older were used in all experiments and performed in accordance to QIMR Berghofer Medical Research Institute animal experimental ethics committee guidelines. The number of mice used in each experimental group was determined on the basis of statistical power analysis to render statistical significance of the experimental data between different experimental groups and ranged from 5 to 12 mice per group. Mice were randomly assigned to different treatment groups. Investigators were blinded to the treatment group received by the mice and assessed the survival of mice without knowing the treatment groups they received. Mice were monitored for symptoms of illness with changes to posture, activity, breathing, and fur texture, and euthanized when clinical symptoms reached the cumulative limit outlined by animal ethics. The number of biological replicates and number of independently performed experiments are indicated in the figure legends. Mouse exclusion criteria were predetermined as follows: 4T1.2-bearing mice were excluded if mice were culled solely because of ethical end points not related to 4T1.2 breast cancer metastases. In flow cytometric analyses, samples containing <20 gp70-tetramer$^+$ CD8$^+$ T cell events were excluded from downstream analyses.

Patient characteristics and tumor sample processing

Resected tumor samples were collected from patients with cancer undergoing surgical treatment for melanoma, non–small cell lung cancer, ovarian cancer, and renal cell carcinoma between April 2017 and October 2020 at the Netherlands Cancer Institute (NKI-AVL), The Netherlands (table S3). The study was approved by the institutional review board of the NKI-AVL (CFMPB484) and executed in compliance with the ethical regulations. All patients consented to the research usage of material not required for diagnostics either by opt-out procedure or via prior informed consent (after 23 May 2018). Pretreatment tumor biopsies were collected from patients enrolled in the PRADO extension cohort of the OpACIN-neo trial (NCT02977052) (7) after obtaining written informed consent (tables S1 and S2).

Resected tumor samples were collected in a medium on ice [RPMI 1640 (Thermo Fisher Scientific) supplemented with 2.5% fetal bovine serum (FBS) (Sigma-Aldrich), 1% penicillin-streptomycin (Roche)]. Tumor samples were immediately dissected into fragments (PDTFs) of 1 to 2 mm^3 on ice. PDTFs from different tumor areas were mixed and frozen in 1 ml of freezing medium [FBS with 10% dimethyl sulfoxide (Sigma-Aldrich)]. Vials were cryopreserved in liquid nitrogen until usage. Tumor biopsies were processed in the same manner as resection samples. Pathological response upon neoadjuvant immunotherapy was assessed by a pathologist according to the INMC scoring system (20).

RNA isolation and NanoString data analysis

RNA was isolated from patients who had sufficient tumor material, based on the pathologist's scoring (at least 30% tumor cells of hematoxylin and eosin–stained cryostat frozen section), in the frozen tumor samples. RNA was simultaneously isolated from fresh-frozen pretreatment tumor frozen sections (10 μm) with the AllPrep DNA/RNA/miRNA Universal Isolation Kit (Qiagen, 80224) using the QIAcube, according to the manufacturer's protocol. Gene expression analysis was conducted using the NanoString nCounter Analysis System and the PanCancer Immune Profiling panel, which captures the read counts of 784 genes (NanoString Technologies, Seattle, WA, USA). Raw counts were normalized to internal expression

of 38 reference genes: *ABCF1*, *AGK*, *ALAS1*, *AMMECR1L*, *CC2D1B*, *CNOT10*, *CNOT4*, *COG7*, *DDX50*, *DHX16*, *EDC3*, *EIF2B4*, *ERCC3*, *FCF1*, *G6PD*, *GPATCH3*, *GUSB*, *HDAC3*, *HPRT1*, *MRPS5*, *MTMR14*, *NOL7*, *NUBP1*, *POLR2A*, *PPIA*, *PRPF38A*, *SAP130*, *SDHA*, *SF3A3*, *TBP*, *TLK2*, *TMUB2*, *TRIM39*, *TUBB*, *USP39*, *ZC3H14*, *ZKSCAN5*, and *ZNF143*. A background count was estimated using the average count of the eight negative control probes in every reaction plus 2 SDs. Next, the CD4/IL-2, CD8 (Danaher), and BATF3 subset gene signature scores were calculated from the average z score of all the genes within each signature separately per patient. The optimal cutoff to determine patients with CD8/BATF3 high or low signature score was computed by the summary receiver operating characteristic (sROC) curves for each signature independently on PRADO and OpACIN-neo cohorts together ($n = 143$). Pearson's correlation method was used to compute the correlation coefficients.

PDTF cultures

PDTF cultures were performed as described previously (23). Briefly, cryo-preserved PDTFs were thawed, extensively washed with wash medium [Dulbecco's modified Eagle's medium (DMEM) supplemented with 10% FBS and 1% penicillin-streptomycin], and embedded in an artificial extracellular matrix {sodium bicarbonate (1.1%; Sigma-Aldrich), collagen I (1 mg/ml; Corning), Matrigel (4 mg/ml; Matrix High Concentration, Phenol Red-Free, BD Biosciences), tumor medium [DMEM supplemented with 1 mM sodium pyruvate (Sigma-Aldrich), 1× MEM non-essential AA (Sigma-Aldrich), 2 mM L-glutamine (Thermo Fisher Scientific), 10% FBS, and 1% penicillin-streptomycin]} in a flat-bottom 96-well plate. PDTF cultures were topped up with tumor medium supplemented with either anti-PD1 (nivolumab, Bristol-Myers Squibb) at 10 μg/ml, anti-CTLA4 (ipilimumab, Bristol-Myers Squibb) at 10 μg/ml, or 3000 pg/ml (~60 IU/ml) recombinant human IL-2 (rhIL-2, Proleukin, PeproTech) where indicated. The rhIL-2 concentration was chosen on the basis of IL-2 plasma concentrations after subcutaneous rhIL-2 treatment (54, 55). After 48 hours of culture at 37°C, supernatants were collected and immediately frozen at −80°C for subsequent cytokine and chemokine analysis. PDTFs were pooled and subjected to flow analysis for assessment of immune cell activation (see below).

Tissue processing and flow cytometric analysis of human samples

PDTFs were collected in 2 ml of digestion mix [RPMI 1640 with 1% penicillin-streptomycin, Pulmozyme (12.6 μg/ml) (Roche), and collagenase type IV (1 mg/ml) (Sigma-Aldrich)] on ice. PDTFs were digested at 37°C while rotating for 45 to 60 min, washed with phosphate-buffered saline (PBS), and filtered. The remaining single-cell suspensions were transferred to a 96-well plate for the staining procedure. Before antibody staining, cells were incubated with human Fc receptor (FcR) Blocking Reagent (eBioscience) for 20 min on ice. Cells were stained with Live/Dead IR Dye (Thermo Fisher Scientific) or Zombie UV (BioLegend) for 20 min on ice, washed, and incubated with the surface antibody mix in fluorescence-activated cell sorting (FACS) buffer [PBS, 0.5% bovine serum albumin (Sigma-Aldrich), and 0.1% NaN$_3$ (Invitrogen)] for 20 min on ice. All antibodies used are listed in table S5. After washing, cells were fixed and permeabilized using the Fix/Perm solution (eBioscience) for 30 min at room temperature. Cells were subsequently washed twice with

1× permeabilization buffer (eBioscience) and incubated with intracellular antibody mix in permeabilization buffer for 40 min at room temperature. Cells were washed twice and resuspended in FACS buffer for data acquisition. For the quantification of immune cell subsets, cells were gated on live (IR Dye negative) and single cells. Cells were identified as nonimmune cells (CD45 negative) and immune cells (CD45$^+$). Within CD3-immune cells, B cells were gated as CD19$^+$, natural killer cells as CD16$^+$, and myeloid cells as CD11b$^+$. T cells were gated as CD3$^+$. These were divided into conventional CD4$^+$ T cells (FOXP3$^-$), T$_{regs}$ (FOXP3$^+$), CD8$^+$ T cells, and natural killer T–like cells (CD16$^+$). For assessment of T cell activation, cells were gated on live (IR Dye negative) and single cells. CD45$^+$CD3$^+$ T cells were subdivided into CD8$^+$, CD4$^+$FOXP3$^-$, and CD4$^+$FOXP3$^+$ T cell subsets. Within each subset, CD137 and OX40 expressions were quantified. Flow cytometric analyses were performed using an LSR II SORP and BD LSRFortessa (BD Bioscience). FlowJo analysis software (v10.6.2) was used for data analysis.

Analysis of cytokines and chemokines and cytotoxic mediators

Supernatants collected from PDTF cultures were thawed on ice and pooled for each experimental condition. The presence of indicated cytokines and chemokines was detected using the LEGENDplex Human Th Cytokine and Human Proinflammatory Chemokine panels (both BioLegend). Cytotoxic mediators were measured using the LEGENDplex Human CD8/NK panel (BioLegend). All assays were performed according to the manufacturer's protocol.

Mice

BALB/c WT and BALB/c Batf3-deficient mice were bred and maintained at the QIMR Berghofer Medical Research Institute. Female mice 8 weeks and older were used in all experiments and performed in accordance to QIMR Berghofer Medical Research Institute animal experimental ethics committee guidelines.

Cell line

BALB/c-derived 4T1.2 mammary carcinomas were maintained in RPMI supplemented with 10% FBS, penicillin/streptomycin, and additional L-glutamine (Gibco) as previously described (3). All cell lines were routinely tested as negative for mycoplasma. Cell line authentication was not routinely performed.

Experimental tumor model

After 4T1.2 orthotopic tumor inoculation into the mammary fat pad and before extensive primary tumor growth, mice develop a substantial burden of metastases in the lungs, liver, bones, and brain, among other organs (3). Female BALB/c WT mice were injected in the fourth or fifth mammary fat pad with 5×10^4 4T1.2 cells. Before the surgical resection of the primary tumor and tumor draining lymph node as previously described (3), mice were treated intraperitoneally with 200 μg of rat control IgG2a (1-1) or a combination of 100 μg of anti-PD1 (RMP1-14), 100 μg of anti-CTLA4 (UC10-4F10-11), and 50,000 IU of rhIL-2 (Proleukin S) (see table S6 for reference). For immune cell depletion experiments, mice were additionally treated with cIg (1-1), anti-CD4 (GK1.5), or anti-CD8β (53-5.8) as indicated in the figure legends. Mice were monitored for symptoms of illness with changes to posture, activity, breathing, and fur texture and euthanized when clinical symptoms reached the cumulative limit outlined by animal ethics. Mice were randomly assigned to treatment groups. All experiments were performed and analyzed double blinded as indicated in the figure legends.

Flow cytometry (mouse)

Tumors, blood, spleen, and draining lymph nodes were harvested from mice and processed for flow cytometry analysis as previously described (27). For surface staining, tumor-infiltrating lymphocyte or immune cell suspensions were stained with antibodies and respective isotype antibodies in the presence of anti-CD16/32 (2.4G2) to block FcR. The list of flow cytometry antibodies used is described in table S6. To stain for Ki67 and FoxP3, samples were fixed and permeabilized with the FOXP3 Fixation/Permeabilization Kit (eBioscience). To measure intracellular cytokine staining, single-cell suspensions were incubated for 5 hours in complete RPMI with monensin and brefeldin A (eBioscience). Samples were then surface stained before being fixed/permeabilized (BD CytoFix/CytoPerm Kit) and stained with anti–IFN-γ, anti-TNF, and anti–IL-2. All data were collected on an LSR Fortessa (Becton Dickinson) flow cytometer and analyzed with FlowJo v10 software (Tree Star Inc.). Gating strategy is shown in figs. S4 and S8.

Statistical analysis

Mouse

Statistical analysis was performed using GraphPad Prism software v.9. Differences between indicated mouse groups were determined by two-way analysis of variance (ANOVA) (or mixed effects analysis when appropriate) test with Tukey's correction as indicated. Differences between survival curves were determined using a log-rank test. P values were considered significant with $P < 0.05$ indicated with (*), $P < 0.01$ with (**), $P < 0.001$ with (***), and $P < 0.0001$ with (****). For all studies, biological replicates and number of independently performed experiments are indicated in the figure legends. Mouse exclusion criteria were predetermined as follows: 4T1.2-bearing mice were excluded if mice were culled solely because of ethical end points not related to 4T1.2 breast cancer metastases. In flow cytometric analyses, samples containing <20 gp70-tetramer$^+$ CD8$^+$ T cell events were excluded from downstream analyses (Fig. 5, B and D, and figs. S5, A and B, S9A, and S11, A to C).

Human

Statistical analysis was performed using GraphPad Prism software v.9. Differences between indicated treatment groups were determined by Mann-Whitney test or Kruskal-Wallis test as indicated. P values were considered significant with $P < 0.05$ indicated with (*), $P < 0.01$ with (**), $P < 0.001$ with (***), and $P < 0.0001$ with (****). Sample size was described for each test separately and on the basis of the availability of patient samples for the analysis. Identification of PDTF responder and nonresponder groups was performed using the built-in unsupervised clustering function in R (v4.0.2). Response patterns in each group were validated in an independent replicate PDTF culture. The IL-2 response score was developed by first calculating receiver operating characteristic (ROC) curves based on the delta values for each parameter measured in the pooled dataset of responders and nonresponders to the anti-CTLA4 + anti-PD1 combination and the anti-CTLA4 + anti-PD1 + IL-2 triple combination. Seven parameters that were strongly discriminative between responders and nonresponders were selected on the basis of the area under the ROC curve. For each parameter, a cutoff value was identified aiming for high specificity and sensitivity. This cutoff was used to score each parameter in each sample depending on whether

Kaptein *et al.*, *Sci. Transl. Med.* **14**, eabj9779 (2022)   27 April 2022

12 of 15

the delta value was above or below the cutoff. The response score was calculated as follows

$$\text{IL} - 2\ \text{response score}\ =\ \frac{\sum \text{All parameters}}{\text{Maximal score}} \times 100$$

SUPPLEMENTARY MATERIALS

www.science.org/doi/10.1126/scitranslmed.abj9779
Figs. S1 to S14
Tables S1 to S6
Data files S1 and S2
MDAR Reproducibility Checklist
View/request a protocol for this paper from *Bio-protocol*.

REFERENCES AND NOTES

1. J. M. Versluis, G. V. Long, C. U. Blank, Learning from clinical trials of neoadjuvant checkpoint blockade. *Nat. Med.* **26**, 475–484 (2020).
2. C. U. Blank, J. B. Haanen, A. Ribas, T. N. Schumacher, CANCER IMMUNOLOGY. The "cancer immunogram". *Science* **352**, 658–660 (2016).
3. J. Liu, S. J. Blake, M. C. Yong, H. Harjunpaa, S. F. Ngiow, K. Takeda, A. Young, J. S. O'Donnell, S. Allen, M. J. Smyth, M. W. Teng, Improved efficacy of neoadjuvant compared to adjuvant immunotherapy to eradicate metastatic disease. *Cancer Discov.* **6**, 1382–1399 (2016).
4. C. U. Blank, E. A. Rozeman, L. F. Fanchi, K. Sikorska, B. van de Wiel, P. Kvistborg, O. Krijgsman, M. van den Braber, D. Philips, A. Broeks, J. V. van Thienen, H. A. Mallo, S. Adriaansz, S. Ter Meulen, L. M. Pronk, L. G. Grijpink-Ongering, A. Bruining, R. M. Gittelman, S. Warren, H. van Tinteren, D. S. Peeper, J. Haanen, A. C. J. van Akkooi, T. N. Schumacher, Neoadjuvant versus adjuvant ipilimumab plus nivolumab in macroscopic stage III melanoma. *Nat. Med.* **24**, 1655–1661 (2018).
5. A. C. Huang, R. J. Orlowski, X. Xu, R. Mick, S. M. George, P. K. Yan, S. Manne, A. A. Kraya, B. Wubbenhorst, L. Dorfman, K. D'Andrea, B. M. Wenz, S. Liu, L. Chilukuri, A. Kozlov, M. Carberry, L. Giles, M. W. Kier, F. Quagliarello, S. McGettigan, K. Kreider, L. Annamalai, Q. Zhao, R. Mogg, W. Xu, W. M. Blumenschein, J. H. Yearley, G. P. Linette, R. K. Amaravadi, L. M. Schuchter, R. S. Herati, B. Bengsch, K. L. Nathanson, M. D. Farwell, G. C. Karakousis, E. J. Wherry, T. C. Mitchell, A single dose of neoadjuvant PD-1 blockade predicts clinical outcomes in resectable melanoma. *Nat. Med.* **25**, 454–461 (2019).
6. R. N. Amaria, S. M. Reddy, H. A. Tawbi, M. A. Davies, M. I. Ross, I. C. Glitza, J. N. Cormier, C. Lewis, W. J. Hwu, E. Hanna, A. Diab, M. K. Wong, R. Royal, N. Gross, R. Weber, S. Y. Lai, R. Ehlers, J. Blando, D. R. Milton, S. Woodman, R. Kageyama, D. K. Wells, P. Hwu, S. P. Patel, A. Lucci, A. Hessel, J. E. Lee, J. Gershenwald, L. Simpson, E. M. Burton, L. Posada, L. Haydu, L. Wang, S. Zhang, A. J. Lazar, C. W. Hudgens, V. Gopalakrishnan, A. Reuben, M. C. Andrews, C. N. Spencer, V. Prieto, P. Sharma, J. Allison, M. T. Tetzlaff, J. A. Wargo, Neoadjuvant immune checkpoint blockade in high-risk resectable melanoma. *Nat. Med.* **24**, 1649–1654 (2018).
7. E. A. Rozeman, A. M. Menzies, A. C. J. van Akkooi, C. Adhikari, C. Bierman, B. A. van de Wiel, R. A. Scolyer, O. Krijgsman, K. Sikorska, H. Eriksson, A. Broeks, J. V. van Thienen, A. D. Guminski, A. T. Acosta, S. Ter Meulen, A. M. Koenen, L. J. W. Bosch, K. Shannon, L. M. Pronk, K. Ch'ng, L. G. G.-Ongering, J. Stretch, S. Heijmink, H. van Tinteren, J. Haanen, O. E. Nieweg, W. M. C. Klop, C. L. Zuur, R. P. M. Saw, W. J. van Houdt, D. S. Peeper, A. J. Spillane, J. Hansson, T. N. Schumacher, G. V. Long, C. U. Blank, Identification of the optimal combination dosing schedule of neoadjuvant ipilimumab plus nivolumab in macroscopic stage III melanoma (OpACIN-neo): A multicentre, phase 2, randomised, controlled trial. *Lancet Oncol.* **20**, 948–960 (2019).
8. C. U. Blank, I. L. M. Reijers, T. Pennington, J. M. Versluis, R. P. Saw, E. A. Rozeman, E. Kapiteijn, A. A. M. V. D. Veldt, K. Suijkerbuijk, G. Hospers, W. M. C. Klop, K. Sikorska, J. A. V. D. Hage, D. J. Grunhagen, A. Spillane, R. V. Rawson, B. A. V. D. Wiel, A. M. Menzies, A. C. J. V. Akkooi, G. V. Long, First safety and efficacy results of PRADO: A phase II study of personalized response-driven surgery and adjuvant therapy after neoadjuvant ipilimumab (IPI) and nivolumab (NIVO) in resectable stage III melanoma. *J. Clin. Oncol.* **38**, 10002 (2020).
9. A. M. Menzies, R. N. Amaria, E. A. Rozeman, A. C. Huang, M. T. Tetzlaff, B. A. van de Wiel, S. Lo, A. A. Tarhini, E. M. Burton, T. E. Pennington, R. P. M. Saw, X. Xu, G. C. Karakousis, P. A. Ascierto, A. J. Spillane, A. C. J. van Akkooi, M. A. Davies, T. C. Mitchell, H. A. Tawbi, R. A. Scolyer, J. A. Wargo, C. U. Blank, G. V. Long, Pathological response and survival with neoadjuvant therapy in melanoma: A pooled analysis from the International Neoadjuvant Melanoma Consortium (INMC). *Nat. Med.* **27**, 301–309 (2021).
10. E. A. Rozeman, E. P. Hoefsmit, I. L. M. Reijers, R. P. M. Saw, J. M. Versluis, O. Krijgsman, P. Dimitriadis, K. Sikorska, B. A. van de Wiel, H. Eriksson, M. Gonzalez, A. T. Acosta, L. G. G.-Ongering, K. Shannon, J. Haanen, J. Stretch, S. Ch'ng, O. E. Nieweg, H. A. Mallo, S. Adriaansz, R. M. Kerkhoven, S. Cornelissen, A. Broeks, W. M. C. Klop, C. L. Zuur, W. J. van Houdt, D. S. Peeper, A. J. Spillane, A. C. J. van Akkooi, R. A. Scolyer, T. N. M. Schumacher, A. M. Menzies, G. V. Long, C. U. Blank, Survival and biomarker analyses

11. from the OpACIN-neo and OpACIN neoadjuvant immunotherapy trials in stage III melanoma. *Nat. Med.* **27**, 256–263 (2021).
11. E. A. Rozeman, L. Fanchi, A. C. J. van Akkooi, P. Kvistborg, J. V. Thienen, B. Stegenga, B. Lamon, J. B. Haanen, T. N. M. Schumacher, C. U. Blank, paper presented at the 42nd ESMO Congress, Madrid, Spain, 8 to 12 September 2017.
12. J. Liu, E. A. Rozeman, J. S. O'Donnell, S. Allen, L. Fanchi, M. J. Smyth, C. U. Blank, M. W. L. Teng, Batf3+ DCs and type I IFN are critical for the efficacy of neoadjuvant cancer immunotherapy. *Oncoimmunology* **8**, e1546068 (2019).
13. J. Borst, T. Ahrends, N. Babala, C. J. M. Melief, W. Kastenmuller, CD4+ T cell help in cancer immunology and immunotherapy. *Nat. Rev. Immunol.* **18**, 635–647 (2018).
14. W. Liao, J. X. Lin, W. J. Leonard, Interleukin-2 at the crossroads of effector responses, tolerance, and immunotherapy. *Immunity* **38**, 13–25 (2013).
15. P. Loetscher, M. Seitz, M. Baggiolini, B. Moser, Interleukin-2 regulates CC chemokine receptor expression and chemotactic responsiveness in T lymphocytes. *J. Exp. Med.* **184**, 569–577 (1996).
16. M. E. Raeber, R. A. Rosalia, D. Schmid, U. Karakus, O. Boyman, Interleukin-2 signals converge in a lymphoid-dendritic cell pathway that promotes anticancer immunity. *Sci. Transl. Med.* **12**, eaba5464 (2020).
17. K. D. Moynihan, C. F. Opel, G. L. Szeto, A. Tzeng, E. F. Zhu, J. M. Engreitz, R. T. Williams, K. Rakhra, M. H. Zhang, A. M. Rothschilds, S. Kumari, R. L. Kelly, B. H. Kwan, W. Abraham, K. Hu, N. K. Mehta, M. J. Kauke, H. Suh, J. R. Cochran, D. A. Lauffenburger, K. D. Wittrup, D. J. Irvine, Eradication of large established tumors in mice by combination immunotherapy that engages innate and adaptive immune responses. *Nat. Med.* **22**, 1402–1410 (2016).
18. N. Zacharakis, H. Chinnasamy, M. Black, H. Xu, Y. C. Lu, Z. Zheng, A. Pasetto, M. Langhan, T. Shelton, T. Prickett, J. Gartner, L. Jia, K. Trebska-McGowan, R. P. Somerville, P. F. Robbins, S. A. Rosenberg, S. L. Goff, S. A. Feldman, Immune recognition of somatic mutations leading to complete durable regression in metastatic breast cancer. *Nat. Med.* **24**, 724–730 (2018).
19. L. S. Cheung, J. Fu, P. Kumar, A. Kumar, M. E. Urbanowski, E. A. Ihms, S. Parveen, C. K. Bullen, G. J. Patrick, R. Harrison, J. R. Murphy, D. M. Pardoll, W. R. Bishai, Second-generation IL-2 receptor-targeted diphtheria fusion toxin exhibits antitumor activity and synergy with anti-PD-1 in melanoma. *Proc. Natl. Acad. Sci. U.S.A.* **116**, 3100–3105 (2019).
20. M. T. Tetzlaff, J. L. Messina, J. E. Stein, X. Xu, R. N. Amaria, C. U. Blank, B. A. van de Wiel, P. M. Ferguson, R. V. Rawson, M. I. Ross, A. J. Spillane, J. E. Gershenwald, R. P. M. Saw, A. C. J. van Akkooi, W. J. van Houdt, T. C. Mitchell, A. M. Menzies, G. V. Long, J. A. Wargo, M. A. Davies, V. G. Prieto, J. M. Taube, R. A. Scolyer, Pathological assessment of resection specimens after neoadjuvant therapy for metastatic melanoma. *Ann. Oncol.* **29**, 1861–1868 (2018).
21. P. Danaher, S. Warren, L. Dennis, L. D'Amico, A. White, M. L. Disis, M. A. Geller, K. Odunsi, J. Beechem, S. P. Fling, Gene expression markers of tumor infiltrating leukocytes. *J. Immunother. Cancer* **5**, 18 (2017).
22. S. Spranger, D. Dai, B. Horton, T. F. Gajewski, Tumor-residing Batf3 dendritic cells are required for effector T cell trafficking and adoptive T cell therapy. *Cancer Cell* **31**, 711–723. e4 (2017).
23. P. Voabil, M. de Bruijn, L. M. Roelofsen, S. H. Hendriks, S. Brokamp, M. van den Braber, A. Broeks, J. Sanders, P. Herzig, A. Zippelius, C. U. Blank, K. J. Hartemink, K. Monkhorst, J. Haanen, T. N. Schumacher, D. S. Thommen, An ex vivo tumor fragment platform to dissect response to PD-1 blockade in cancer. *Nat. Med.* **27**, 1250–1261 (2021).
24. A. K. Abbas, E. Trotta, D. R. Simeonov, A. Marson, J. A. Bluestone, Revisiting IL-2: Biology and therapeutic prospects. *Sci. Immunol.* **3**, eaat1482 (2018).
25. J. P. Dutcher, D. J. Schwartzentruber, H. L. Kaufman, S. S. Agarwala, A. A. Tarhini, J. N. Lowder, M. B. Atkins, High dose interleukin-2 (Aldesleukin)—Expert consensus on best management practices-2014. *J. Immunother. Cancer* **2**, 26 (2014).
26. M. Ahmadzadeh, S. A. Rosenberg, IL-2 administration increases CD4+ CD25(hi) Foxp3+ regulatory T cells in cancer patients. *Blood* **107**, 2409–2414 (2006).
27. J. Liu, J. S. O'Donnell, J. Yan, J. Madore, S. Allen, M. J. Smyth, M. W. L. Teng, Timing of neoadjuvant immunotherapy in relation to surgery is crucial for outcome. *Oncoimmunology* **8**, e1581530 (2019).
28. N. S. Joshi, W. Cui, A. Chandele, H. K. Lee, D. R. Urso, J. Hagman, L. Gapin, S. M. Kaech, Inflammation directs memory precursor and short-lived effector CD8+ T cell fates via the graded expression of T-bet transcription factor. *Immunity* **27**, 281–295 (2007).
29. C. Gerlach, E. A. Moseman, S. M. Loughhead, D. Alvarez, A. J. Zwijnenburg, L. Waanders, R. Garg, J. C. de la Torre, U. H. von Andrian, The chemokine receptor CX3CR1 defines three antigen-experienced CD8 T cell subsets with distinct roles in immune surveillance and homeostasis. *Immunity* **45**, 1270–1284 (2016).
30. M. J. Selby, J. J. Engelhardt, M. Quigley, K. A. Henning, T. Chen, M. Srinivasan, A. J. Korman, Anti-CTLA-4 antibodies of IgG2a isotype enhance antitumor activity through reduction of intratumoral regulatory T cells. *Cancer Immunol. Res.* **1**, 32–42 (2013).
31. J. E. Gershenwald, R. A. Scolyer, K. R. Hess, V. K. Sondak, G. V. Long, M. I. Ross, A. J. Lazar, M. B. Faries, J. M. Kirkwood, G. A. McArthur, L. E. Haydu, A. M. M. Eggermont, K. T. Flaherty,

Kaptein *et al.*, *Sci. Transl. Med.* **14**, eabj9779 (2022)   27 April 2022

13 of 15

C. M. Balch, J. F. Thompson, Melanoma staging: Evidence-based changes in the American Joint Committee on Cancer eighth edition cancer staging manual. *CA Cancer J. Clin.* **67**, 472–492 (2017).

32. A. C. van Akkooi, M. G. Bouwhuis, A. N. van Geel, R. Hoedemaker, C. Verhoef, D. J. Grunhagen, P. I. Schmitz, A. M. Eggermont, J. H. de Wilt, Morbidity and prognosis after therapeutic lymph node dissections for malignant melanoma. *Eur. J. Surg. Oncol.* **33**, 102–108 (2007).

33. A. P. van der Ploeg, A. C. van Akkooi, P. I. Schmitz, A. N. van Geel, J. H. de Wilt, A. M. Eggermont, C. Verhoef, Therapeutic surgical management of palpable melanoma groin metastases: Superficial or combined superficial and deep groin lymph node dissection. *Ann. Surg. Oncol.* **18**, 3300–3308 (2011).

34. I. L. M. Reijers, P. Dimitriadis, E. A. Rozeman, J. M. Versluis, A. Broeks, L. J. W. Bosch, J. Bouwman, S. Cornelissen, O. Krijgsman, M. Gonzalez, D. S. Rao, L. G. Grijpink-Ongering, M. van Dijk, A. Spillane, R. A. Scolyer, B. A. Van de Wiel, A. M. Menzies, A. C. J. Van Akkooi, G. V. Long, C. U. Blank, paper presented at the ASCO Virtual Scientific Program, Chicago, IL, 29 to 31 May 2020.

35. P. E. Kovanen, L. Young, A. Al-Shami, V. Rovella, C. A. Pise-Masison, M. F. Radonovich, J. Powell, J. Fu, J. N. Brady, P. J. Munson, W. J. Leonard, Global analysis of IL-2 target genes: Identification of chromosomal clusters of expressed genes. *Int. Immunol.* **17**, 1009–1021 (2005).

36. R. Akbani, K. C. Akdemir, B. A. Aksoy, M. Albert, A. Ally, S. B. Amin, H. Arachchi, A. Arora, J. T. Auman, B. Ayala, J. Baboud, M. Balasundaram, S. Balu, N. Barnabas, J. Bartlett, P. Bartlett, B. C. Bastian, S. B. Baylin, M. Behera, D. Belyaev, C. Benz, B. Bernard, R. Beroukhim, N. Bir, A. D. Black, T. Bodenheimer, L. Boice, G. M. Boland, R. Bono, M. S. Bootwalla, M. Bosenberg, J. Bowen, R. Bowlby, C. A. Bristow, L. B.-Lunardi, D. Brooks, J. Brzezinski, W. Bshara, E. Buda, W. R. Burns, Y. S. N. Butterfield, M. Button, T. Calderone, G. A. Cappellini, C. Carter, S. L. Carter, L. Cherney, A. D. Cherniack, A. Chevalier, L. Chin, J. Cho, R. J. Cho, Y.-L. Choi, A. Chu, S. Chudamani, K. Cibulskis, G. Ciriello, A. Clarke, S. Coons, L. Cope, D. Crain, E. Curley, L. Danilova, S. D'Atri, T. Davidsen, M. A. Davies, K. A. Delman, J. A. Demchok, Q. A. Deng, Y. L. Deribe, N. Dhalla, R. Dhir, D. DiCara, A. Dinikin, M. Dubina, J. S. Ebrom, S. Egea, G. Eley, J. Engel, J. M. Eschbacher, K. V. Fedosenko, I. Felau, T. Fennell, M. L. Ferguson, S. Fisher, K. T. Flaherty, S. Frazer, J. Frick, V. Fulidou, S. B. Gabriel, J. Gao, J. Gardner, L. A. Garraway, J. M. Gastier-Foster, C. Gaudioso, N. Gehlenborg, G. Genovese, M. Gerken, J. E. Gershenwald, C. Getz, C. Gomez-Fernandez, T. Gribbin, J. Grimsby, B. Gross, R. Guin, T. Gutschner, A. Hadjipanayis, R. Halaban, B. Hanf, D. Haussler, L. E. Haydu, D. N. Hayes, N. K. Hayward, D. I. Heiman, L. Herbert, J. G. Herman, P. Hersey, K. A. Hoadley, E. Hodis, R. A. Holt, D. S. Hoon, S. Hoppough, A. P. Hoyle, F. W. Huang, M. Huang, S. Huang, C. M. Hutter, M. Ibbs, L. Iype, A. Jacobsen, V. Jakrot, A. Janning, W. R. Jeck, S. R. Jefferys, M. A. Jensen, C. D. Jones, S. J. M. Jones, Z. Ju, H. Kakavand, H. Kang, R. F. Kefford, F. R. Khuri, J. Kim, J. M. Kirkwood, J. Klode, A. Korkut, K. Korski, M. Krauthammer, R. Kucherlapati, L. N. Kwong, M. Kycler, M. Ladanyi, P. H. Lai, P. W. Laird, E. Lander, M. S. Lawrence, A. J. Lazar, R. Łaźniak, D. Lee, J. E. Lee, J. Lee, K. Lee, S. Lee, W. Lee, E. Leporowska, K. M. Leraas, H. I. Li, T. M. Lichtenberg, L. Lichtenstein, P. Lin, S. Ling, J. Liu, O. Liu, W. Liu, G. V. Long, Y. Lu, S. Ma, Y. Ma, A. Mackiewicz, H. S. Mahadeshwar, J. Malke, D. Mallery, G. M. Manikhas, G. J. Mann, M. A. Marra, B. Matejka, M. Mayo, S. Mehrabi, S. Meng, M. Meyerson, P. A. Mieczkowski, J. P. Miller, M. L. Miller, G. B. Mills, F. Moiseenko, R. A. Moore, S. Morris, C. Morrison, D. Morton, S. Moschos, L. E. Mose, F. L. Muller, A. J. Mungall, D. Murawa, P. Murawa, B. A. Murray, L. Nezi, S. Ng, D. Nicholson, M. S. Noble, A. Osunkoya, T. K. Owonikoko, B. A. Ozenberger, E. Pagani, O. V. Paklina, A. Pantazi, M. Parfenov, J. Parfitt, P. J. Park, W.-Y. Park, J. S. Parker, F. Passarelli, R. Penny, C. M. Perou, T. D. Pihl, O. Potapova, V. G. Prieto, A. Protopopov, M. J. Quinn, A. Radenbaugh, K. Rai, S. S. Ramalingam, A. T. Raman, N. C. Ramirez, R. Ramirez, U. Rao, W. K. Rathmell, X. Ren, S. M. Reynolds, J. Roach, A. G. Robertson, M. I. Ross, J. Roszik, G. Russo, G. P. Saksena, C. Saller, Y. Samuels, C. Sander, C. Sander, G. Sandusky, N. Santoso, M. Saul, R. P. Saw, D. Schadendorf, J. E. Schein, N. Schultz, S. E. Schumacher, C. Schwallier, R. A. Scolyer, J. Seidman, P. C. Sekhar, H. S. Sekhon, Y. Senbabaoglu, S. Seth, K. F. Shannon, S. Sharpe, N. E. Sharpless, K. R. M. Shaw, C. Shelton, T. Shelton, R. Shen, M. Sheth, Y. Shi, C. J. Shiau, I. Shmulevich, G. L. Sica, J. V. Simons, R. Sinha, P. Sipahimalani, H. J. Sofia, M. G. Soloway, X. Song, C. Sougnez, A. J. Spillane, A. Spychała, J. R. Stretch, J. Stuart, W. M. Suchorska, A. Sucker, S. O. Sumer, Y. Sun, M. Synott, B. Tabak, T. R. Tabler, A. Tam, D. Tan, J. Tang, R. Tarnuzzer, K. Tarvin, H. Tatka, B. S. Taylor, M. Teresiak, N. Thiessen, J. F. Thompson, L. Thorne, V. Thorsson, J. M. Trent, T. J. Triche, K. Y. Tsai, P. Tsou, D. J. Van Den Berg, E. M. Van Allen, U. Veluvolu, R. G. Verhaak, D. Voet, O. Voronina, V. Walter, J. S. Walton, Y. Wan, Y. Wang, Z. Wang, S. Waring, I. R. Watson, N. Weinhold, J. N. Weinstein, D. J. Weisenberger, P. White, M. D. Wilkerson, J. S. Wilmott, L. Wise, M. Wiznerowicz, S. E. Woodman, C.-J. Wu, C.-C. Wu, J. Wu, Y. Wu, X. Xi, A. W. Xu, D. Yang, L. Yang, L. Yang, T. I. Zack, J. C. Zenklusen, H. Zhang, J. Zhang, W. Zhang, X. Zhao, J. Zhu, K. Zhu, L. Zimmer, E. Zmuda, L. Zou, Genomic classification of cutaneous melanoma. *Cell* **161**, 1681–1696 (2015).

37. D. Sahin, N. Arenas-Ramirez, M. Rath, U. Karakus, M. Humbelin, M. van Gogh, L. Borsig, O. Boyman, An IL-2-grafted antibody immunotherapy with potent efficacy against metastatic cancer. *Nat. Commun.* **11**, 6440 (2020).

38. E. B. Wilson, A. M. Livingstone, Cutting edge: CD4⁺ T cell-derived IL-2 is essential for help-dependent primary CD8⁺ T cell responses. *J. Immunol.* **181**, 7445–7448 (2008).

39. M. A. Gavin, T. R. Torgerson, E. Houston, P. DeRoos, W. Y. Ho, A. Stray-Pedersen, E. L. Ocheltree, P. D. Greenberg, H. D. Ochs, A. Y. Rudensky, Single-cell analysis of normal and FOXP3-mutant human T cells: FOXP3 expression without regulatory T cell development. *Proc. Natl. Acad. Sci. U.S.A.* **103**, 6659–6664 (2006).

40. M. E. Morgan, J. H. van Bilsen, A. M. Bakker, B. Heemskerk, M. W. Schilham, F. C. Hartgers, B. G. Elferink, L. van der Zanden, R. R. de Vries, T. W. Huizinga, T. H. Ottenhoff, R. E. Toes, Expression of FOXP3 mRNA is not confined to CD4⁺CD25⁺ T regulatory cells in humans. *Hum. Immunol.* **66**, 13–20 (2005).

41. J. M. Kim, J. P. Rasmussen, A. Y. Rudensky, Regulatory T cells prevent catastrophic autoimmunity throughout the lifespan of mice. *Nat. Immunol.* **8**, 191–197 (2007).

42. A. E. O.-Delgoffe, M. Chikina, R. E. Dadey, H. Yano, E. A. Brunazzi, G. Shayan, W. Horne, J. M. Moskovitz, J. K. Kolls, C. Sander, Y. Shuai, D. P. Normolle, J. M. Kirkwood, R. L. Ferris, G. M. Delgoffe, T. C. Bruno, C. J. Workman, D. A. A. Vignali, Interferon-γ drives T$_{reg}$ fragility to promote anti-tumor immunity. *Cell* **169**, 1130–1141.e11 (2017).

43. J. M. Drerup, Y. Deng, S. L. Pandeswara, A. S. Padron, R. M. Reyes, X. Zhang, J. Mendez, A. Liu, C. A. Clark, W. Chen, J. R. Conejo-Garcia, V. Hurez, H. Gupta, T. J. Curiel, CD122-selective IL2 complexes reduce immunosuppression, promote treg fragility, and sensitize tumor response to PD-L1 blockade. *Cancer Res.* **80**, 5063–5075 (2020).

44. R. Zappasodi, I. Serganova, I. J. Cohen, M. Maeda, M. Shindo, Y. Senbabaoglu, M. J. Watson, A. Leftin, R. Maniyar, S. Verma, M. Lubin, M. Ko, M. M. Mane, H. Zhong, C. Liu, A. Ghosh, M. Abu-Akeel, E. Ackerstaff, J. A. Koutcher, P. C. Ho, G. M. Delgoffe, R. Blasberg, J. D. Wolchok, T. Merghoub, CTLA-4 blockade drives loss of T$_{reg}$ stability in glycolysis-low tumours. *Nature* **591**, 652–658 (2021).

45. S. A. Lim, J. Wei, T. M. Nguyen, H. Shi, W. Su, G. Palacios, Y. Dhungana, N. M. Chapman, L. Long, J. Saravia, P. Vogel, H. Chi, Lipid signalling enforces functional specialization of Treg cells in tumours. *Nature* **591**, 306–311 (2021).

46. C. Krieg, S. Letourneau, G. Pantaleo, O. Boyman, Improved IL-2 immunotherapy by selective stimulation of IL-2 receptors on lymphocytes and endothelial cells. *Proc. Natl. Acad. Sci. U.S.A.* **107**, 11906–11911 (2010).

47. N. Arenas-Ramirez, C. Zou, S. Popp, D. Zingg, B. Brannetti, E. Wirth, T. Calzascia, J. Kovarik, L. Sommer, G. Zenke, J. Woytschak, C. H. Regnier, A. Katopodis, O. Boyman, Improved cancer immunotherapy by a CD25-mimobody conferring selectivity to human interleukin-2. *Sci. Transl. Med.* **8**, 367ra166 (2016).

48. I. Waldhauer, V. Gonzalez-Nicolini, A. F.-Grundschober, T. K. Nayak, L. Fahrni, R. J. Hosse, D. Gerrits, E. J. W. Geven, J. Sam, S. Lang, E. Bommer, V. Steinhart, E. Husar, S. Colombetti, E. Van Puijenbroek, M. Neubauer, J. M. Cline, P. K. Garg, G. Dugan, F. Cavallo, G. Acuna, J. Charo, V. Teichgraber, S. Evers, O. C. Boerman, M. Bacac, E. Moessner, P. Umana, C. Klein, Simlukafusp alfa (FAP-IL2v) immunocytokine is a versatile combination partner for cancer immunotherapy. *MAbs* **13**, 1913791 (2021).

49. H. Sultan, K. Moynihan, Y. Song, S. Ameh, T. Schumacher, Y. A. Yeung, I. Djuretic, R. Schreiber, 578 CD8-targeted IL-2 drives potent anti-tumor efficacy and promotes action of tumor specific vaccines. *J. Immunother. Cancer* **9**, A607 (2021).

50. Z. Ren, A. Zhang, Z. Sun, Y. Liang, J. Ye, J. Qiao, B. Li, Y. X. Fu, Selective delivery of low-affinity IL-2 to PD-1⁺ T cells rejuvenates antitumor immunity with reduced toxicity. *J. Clin. Invest.* **132**, e153604 (2022).

51. M. Chalabi, L. F. Fanchi, K. K. Dijkstra, J. G. Van den Berg, A. G. Aalbers, K. Sikorska, M. Lopez-Yurda, C. Grootscholten, G. L. Beets, P. Snaebjornsson, M. Maas, M. Mertz, V. Veninga, G. Bounova, A. Broeks, R. G. Beets-Tan, T. R. de Wijkerslooth, A. U. van Lent, H. A. Marsman, E. Nuijten, N. F. Kok, M. Kuiper, W. H. Verbeek, M. Kok, M. E. Van Leerdam, T. N. Schumacher, E. E. Voest, J. B. Haanen, Neoadjuvant immunotherapy leads to pathological responses in MMR-proficient and MMR-deficient early-stage colon cancers. *Nat. Med.* **26**, 566–576 (2020).

52. N. van Dijk, A. Gil-Jimenez, K. Silina, K. Hendricksen, L. A. Smit, J. M. de Feijter, M. L. van Montfoort, C. van Rooijen, D. Peters, A. Broeks, H. G. van der Poel, A. Bruining, Y. Lubeck, K. Sikorska, T. N. Boellaard, P. Kvistborg, D. J. Vis, E. Hooijberg, T. N. Schumacher, M. van den Broek, L. F. A. Wessels, C. U. Blank, B. W. van Rhijn, M. S. van der Heijden, Preoperative ipilimumab plus nivolumab in locoregionally advanced urothelial cancer: The NABUCCO trial. *Nat. Med.* **26**, 1839–1844 (2020).

53. T. Cascone, N. William Jr., A. Weissferdt, C. H. Leung, H. Y. Lin, A. Pataer, M. C. B. Godoy, B. W. Carter, L. Federico, A. Reuben, M. A. W. Khan, H. Dejima, A. Francisco-Cruz, E. R. Parra, L. M. Solis, J. Fujimoto, H. T. Tran, N. Kalhor, F. V. Fossella, F. E. Mott, A. S. Tsao, G. Blumenschein Jr., X. Le, J. Zhang, F. Skoulidis, J. M. Kurie, M. Altan, C. Lu, B. S. Glisson, L. A. Byers, Y. Y. Elamin, R. J. Mehran, D. C. Rice, G. L. Walsh, W. L. Hofstetter, J. A. Roth, M. B. Antonoff, H. Kadara, C. Haymaker, C. Bernatchez, N. J. Ajami, R. R. Jenq, P. Sharma, J. P. Allison, A. Futreal, J. A. Wargo, I. I. Wistuba, S. G. Swisher, J. J. Lee, D. L. Gibbons, A. A. Vaporciyan, J. V. Heymach, B. Sepesi, Neoadjuvant nivolumab or nivolumab plus ipilimumab in operable non-small cell lung cancer: The phase 2 randomized NEOSTAR trial. *Nat. Med.* **27**, 504–514 (2021).

Kaptein *et al.*, *Sci. Transl. Med.* **14**, eabj9779 (2022)   27 April 2022

14 of 15

54. G. I. Kirchner, A. Franzke, J. Buer, W. Beil, M. Probst-Kepper, F. Wittke, K. Overmann, S. Lassmann, R. Hoffmann, H. Kirchner, A. Ganser, J. Atzpodien, Pharmacokinetics of recombinant human interleukin-2 in advanced renal cell carcinoma patients following subcutaneous application. *Br. J. Clin. Pharmacol.* **46**, 5–10 (1998).

55. O. Eton, M. G. Rosenblum, S. S. Legha, W. Zhang, M. Jo East, A. Bedikian, N. Papadopoulos, A. Buzaid, R. S. Benjamin, Phase I trial of subcutaneous recombinant human interleukin-2 in patients with metastatic melanoma. *Cancer* **95**, 127–134 (2002).

56. C. Thiele, G. Hirschfeld, cutpointr: Improved estimation and validation of optimal cutpoints in R. *J. Stat. Softw.* **98**, 1–27 (2021).

Kaptein *et al.*, *Sci. Transl. Med.* **14**, eabj9779 (2022)   27 April 2022

15 of 15

Addition of interleukin-2 overcomes resistance to neoadjuvant CTLA4 and PD1 blockade in ex vivo patient tumors

Paulien Kaptein, Celia Jacoberger-Foissac, Petros Dimitriadis, Paula Voabil, Marjolein de Bruijn, Simone Brokamp, Irene Reijers, Judith Versluis, Gahyathiri Nallan, Hannah Triscott, Elizabeth McDonald, Joshua Tay, Georgina V. Long, Christian U. Blank, Daniela S. Thommen, and Michele W.L. Teng

Immunotherapy triple threat

Some patients with melanoma do not respond to dual immunotherapy of anti-cytotoxic T lymphocyte–associated protein 4 (CTLA4) and anti–programmed cell death protein 1 (PD1). Kaptein *et al.* identified a low interleukin 2 (IL-2) gene signature associated with resistance in patients with melanoma. The addition of IL-2 to dual immunotherapy treatment of resistant ex vivo patient samples and mouse models induced immunological responses and extended survival. Therapy expanded tumor-specific CD8+ T cells and improved proinflammatory cytokine polyfunctionality of T cells in vivo. Triple-combination immunotherapy can overcome resistance to dual neoadjuvant immunotherapy and warrants further testing in patients with early-stage melanoma.

View the article online
https://www.science.org/doi/10.1126/scitranslmed.abj9779
Permissions
https://www.science.org/help/reprints-and-permissions